Title
A Free-Radical Prompted Barrierless Gas-Phase Synthesis of Pentacene

Journal
Angewandte Chemie, 132(28)

ISSN
0044-8249

Authors
Zhao, Long
Kaiser, Ralf I
Lu, Wenchao
et al.

Publication Date
2020-07-06

DOI
10.1002/ange.202003402

Peer reviewed

A Free Radical Prompted Barrierless Gas Phase Synthesis of Pentacene

Long Zhao, Ralf I. Kaiser*

Department of Chemistry, University of Hawaii at Manoa, Honolulu, HI, 96822, USA

Wenchao Lu, Musahid Ahmed*

Chemical Sciences Division, Lawrence Berkeley National Laboratory, Berkeley, CA 94720, USA

Mikhail M. Evseev, Eugene K. Bashkirov

Samara National Research University, Samara 443086, Russian Federation

V. N. Azyazov

Lebedev Physical Institute, Samara 443011
and Samara National Research University, Samara 443086, Russian Federation

Alexander M. Mebel*

Department of Chemistry and Biochemistry, Florida International University, Miami, FL 33199, USA

Christina Tönshoff, Florian Reicherter, Holger F. Bettinger*

Institute of Organic Chemistry, University of Tübingen, Auf der Morgenstelle 18; 72076 Tübingen, Germany

* Corresponding authors:
Prof. Dr. Ralf I. Kaiser <ralfk@hawaii.edu>
Dr. Musahid Ahmed <MAhmed@lbl.gov>
Prof. Dr. Alexander M. Mebel <mebela@fiu.edu>
Prof. Dr. Holger F. Bettinger <holger.bettinger@uni-tuebingen.de>

ABSTRACT: A representative, low temperature gas phase reaction mechanism synthesizing polyacenes via ring annulation exemplified by the formation of pentacene ($C_{22}H_{14}$) along with its benzo[*a*]tetracene isomer ($C_{22}H_{14}$) is unraveled by probing the elementary reaction of the 2-tetracenyl radical ($C_{18}H_{11}^{\bullet}$) with vinylacetylene (C_4H_4). The pathway to pentacene – a prototype polyacene and a fundamental molecular building block in graphenes, fullerenes, and carbon nanotubes – is facilitated by a barrierless, vinylacetylene mediated gas phase chemistry thus disputing conventional hypotheses that synthesis of polycyclic aromatic hydrocarbons (PAHs) solely proceeds at elevated temperatures. This low temperature pathway can launch isomer-selective routes to aromatic structures through submerged reaction barriers, resonantly stabilized free radical intermediates, and methodical ring annulation in deep space eventually changing our perception about the chemistry of carbon in our Universe.

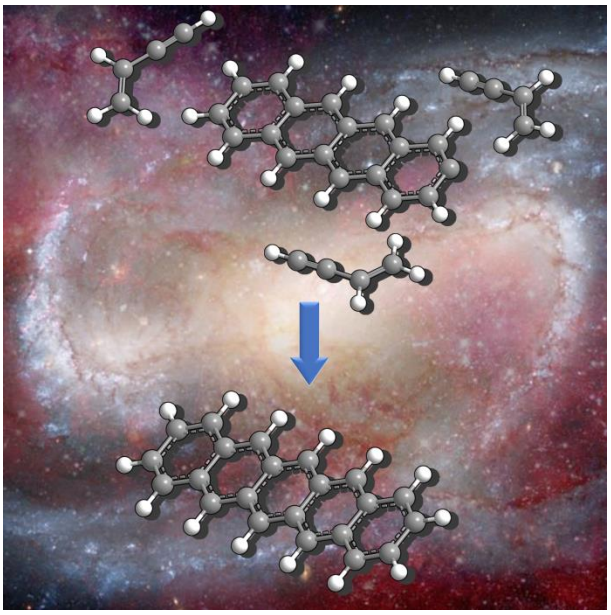

Pentacene can be formed through molecular mass growth processes via ring annulation at low temperatures via the reaction of 2-tetracenyl radicals with vinylacetylene.

Keywords: Hydrogen Abstraction/Vinylacetylene Addition (HAVA) • polycyclic aromatic hydrocarbons • gas-phase chemistry • mass spectrometry • interstellar medium

Since the very first isolation of tetracene ($C_{18}H_{12}$) and pentacene ($C_{22}H_{14}$) by Ernst & Siegmund (1898)[1] and Mills & Gostling (1912) more than a century ago, acenes - polycyclic aromatic hydrocarbons (PAHs) with the molecular formula $C_{4n+2}H_{2n+4}$ ($n \geq 4$) formally grown by linear fusion of benzene molecules[2] (Scheme 1) - have attracted extensive attention from the physical chemistry, organic chemistry, material science, and astrochemistry communities. This interest is based on their exceptional optoelectronic properties - often in combination with Buckminster-fullerene (C_{60}) – as organic semiconductors[3] and organic field effect transistors (OFETs).[4] Acenes also play a fundamental role as molecular building blocks in nanotubes,[5] graphenes,[6] nanoflakes,[7] and fullerenes (C_{70}) (Scheme 2)[8] and have been suggested as potential carriers of (some of) the diffuse interstellar bands (DIBs)[9] - discrete absorption features overlaid on the interstellar extinction curve from the blue part of the visible (400 nm) to the near-infrared (1.2 mm).[10] Structurally, the 22 π-aromatic pentacene ($C_{22}H_{14}$) represents a linear (planar) acene with tetracene ($C_{18}H_{12}$) and hexacene ($C_{26}H_{16}$) defining the previous and next member in the homologous series, respectively. Although unsubstituted acenes hold a D_{2h} point group, substitution by phenyl groups in pentacene distorts the acene moiety out of plane resulting in right- and left-handed enantiomers with end-to-end twists of 144°.[11] Considering the highly reactive 6 and 13 positions of pentacene due to π-electron localization, the aromatic character of pentacene is quite distinct from PAHs such as naphthalene ($C_{10}H_8$). This is evident from the facile oxidation of pentacene at the 6 and 13 positions to pentacene quinone[12] and a tautomeric equilibrium between 6-methylpentacene and 6-methylene-6,13-dihydropentacene favoring the methylene species.[13]

There are a number of ways to synthesize acenes. Classical approaches involve the reduction of acenequinones, the deoxygenation of epoxyacenes, and the dehydrogenation of hydroacenes.[14] More recent techniques are the photo bisdecarbonylation of bridged α-diketones (Strating-Zwanenburg reaction)[15] and the photochemical or thermal extrusion of carbon monoxide, a retro-cheletropic reaction.[16] The latter approaches were exploited successfully for the generation of the largest acenes under matrix isolation conditions and in ultrahigh vacuum on noble metal surfaces: heptacene (n = 7), octacene (n = 8), nonacene (n = 9), and undecacene (n = 11).[17] Based on the absorption spectra, an optical gap of 1.2 eV was extrapolated for the infinitely long polyacene. Nonacene (n = 9), decacene (n = 10), and undecacene (n = 11) were prepared *in situ* on gold surfaces using α-diketone, hydroacene, and epoxyacene precursors. The

HOMO-LUMO gap of undecacene was determined to be only 1.2 eV.[18] However, despite extraordinary progress on the synthesis and characterization of higher acenes, molecular mass growth processes leading to these aromatic molecules at extreme temperatures of 10 K as present in molecular clouds have not been reported yet. A fundamental understanding of these processes is critical not only to constrain the formation of a key class of aromatic compounds – acenes – in deep space (after all, if acenes contribute to the DIBS carriers , they have to be synthesized in the interstellar medium), but also to elucidate non-traditional, low-temperature reaction mechanisms to precursors to carbonaceous nanostructures in interstellar environments eventually bringing us closer to an understanding of the carbon chemistry in our Universe.

In this *Communication,* we report on a pathway to synthesize polyacenes through a targeted, vinylacetylene prompted gas phase chemistry via ring annulation involving bimolecular reactions with aryl radicals. In distinction to aforementioned routes pursuing gas phase pyrolysis of labile precursors,[19] preparative high temperature solution chemistry,[20] and matrix isolation,[21] the novel gas phase synthesis involves a de-facto barrierless reaction via molecular mass growth from the bottom-up via ring addition involving free radical reaction intermediates. Exploiting pentacene as a prototype, we expose the previously unknown gas phase chemistry forming pentacene ($C_{22}H_{14}$; 278 amu) along with atomic hydrogen (1 amu) through the elementary reaction of the 2-tetracenyl radical ($C_{18}H_{11}^{\bullet}$; 227 amu) with vinylacetylene (C_4H_4; 52 amu). Tetracene has been proposed to exist in the interstellar medium (ISM);[9] the 2-tetracenyl radical can be generated from tetracene via photolysis by the internal ultraviolet field existing even deep inside molecular clouds. Laboratory studies have shown that vinylacetylene can be synthesized in deep space via the barrier-less gas phase reaction of ethylene (C_2H_4) with the ethynyl radical (C_2H).[22] Engaging a combination of laboratory experiments and *ab initio* electronic structure calculations, this proof-of-concept study reveals a benchmark of an unconventional, barrierless reaction through resonance-stabilized free radical (RSFR) intermediates ($C_{22}H_{15}^{\bullet}$) leading to an efficient gas phase synthesis of pentacene. This route represents a facile, representative mechanism to systematically build up more complex polyacenes such as hexacene and heptacene through successive ring annulation – one ring at a time – involving bimolecular gas phase reactions of an aryl radical with vinylacetylene. The extracted reaction mechanism also allows a selective design of substituted acenes by replacing hydrogen atoms in the aryl and/or vinyl-acetylene reactant(s) by organic groups thus connecting to substituted acenes, whose classical

synthetic chemistry has been proven challenging. These processes operate even at ultralow interstellar temperatures as low as 10 K hence providing an unconventional synthetic route to potential carriers of DIBs: polyacenes. Briefly, a chemical microreactor was utilized to synthesize pentacene through the gas phase reaction of the 2-tetracenyl radical ($C_{18}H_{11}^{\bullet}$) with vinylacetylene (C_4H_4). The nascent reaction products were sampled in a molecular beam isomer-specifically via fragment-free photoionization of the neutral products exploiting tunable vacuum ultraviolet (VUV) light followed by detection of the ionized molecules in a reflectron time-of-flight mass spectrometer (ReTOFMS) (Supporting Information).

A representative mass spectrum recorded at a photoionization energy of 9.50 eV is displayed in Figure 1 for the reaction of the 2-tetracenyl radical ($C_{18}H_{11}^{\bullet}$; 227 amu) formed via flash pyrolysis of 2-bromotetracene with vinylacetylene (C_4H_4; 52 amu). Control experiments were also carried out by replacing the vinylacetylene reactant with non-reactive helium carrier gas (Figure 1). A comparison of both data sets reveals compelling evidence on the formation of a molecule with the molecular formula $C_{22}H_{14}$ (278 amu) in the 2-tetracenyl – vinylacetylene system (Figure 1b); this signal is absent in the control experiment (Figure 1a). Considering the molecular weight of the reactant molecules and the products, it is evident that the $C_{22}H_{14}$ isomer(s) together with the hydrogen atom are formed via the reaction of the 2-tetracenyl radical with vinylacetylene. Note that signal at m/z = 252 ($C_{20}H_{12}$) is likely linked to 2-ethynyltetracene formed via the reaction of the 2-tetracenyl radical ($C_{18}H_{11}$; 227 amu) with acetylene (C_2H_2; 26 amu) (Supporting Information). Ion counts at mass-to-charge ratios (*m/z*) from 306 to 309 ($C_{18}H_{11}{}^{79}Br^+$, $^{13}CC_{17}H_{11}{}^{79}Br^+$, $C_{18}H_{11}{}^{81}Br^+$, $^{13}CC_{17}H_{11}{}^{79}Br^+$) and from 226 to 229 ($C_{18}H_{10}$, $^{13}CC_{17}H_{10}/C_{18}H_{11}$, $C_{18}H_{12}$, $^{13}CC_{17}H_{10}$) are evident in the 2-tetracenyl – vinylacetylene and helium-vinylacetylene systems; this finding suggests that these molecules are not connected to the gas phase reaction of the 2-tetracenyl radical with vinylacetylene. Here, ion counts at *m/z* = 306 – 309 are connected to the non-pyrolyzed 2-bromotetracene precursor, while signals at m/z = 226 and 227 are associated with $C_{18}H_{10}$ and ^{13}C-$C_{17}H_{10}$ formed via hydrogen abstraction from the 2-tetracenyl radical and its ^{13}C-substittued counterpart. Finally, ion counts at *m/z* = 228 and 229 are likely traced to tetracene and ^{13}C-tetracene, respectively, and/or originate from dissociative photoionization of the precursor (Supporting Information).

With the detection of hydrocarbon molecules holding the molecular formula $C_{22}H_{14}$ formed through reactive collisions of the 2-tetracenyl radical with vinylacetylene, we aim to assign the

structural isomer(s) synthesized in this reaction. This requires an in-depth analysis of the corresponding photoionization efficiency (PIE) curve, which displays the intensity of the ion at *m/z* of 278 ($C_{22}H_{14}^+$) as a function of the photon energy from 6.60 eV to 9.00 eV (Figure 2). This graph could be reproduced through a linear combination of two distinct reference PIE curves of discrete $C_{22}H_{14}$ isomers: pentacene (green) and benzo[*a*]tetracene (blue) (Figure 2). The experimental and reference PIE curves for pentacene show an onset of 6.65 ± 0.05 eV, which agrees nicely with the literature value of the adiabatic ionization energy of 6.61 eV.[23] The addition of the reference PIE curve of benzo[*a*]tetracene significantly improves the fits from 7.20 to 9.0 eV and accounts for 11 ± 5 % in the ion counts. Fitting the experimental data only with pentacene does not reproduce the curve. It is important to highlight that both reference curves were recorded in an identical experimental setup as the 2-tetracenyl – vinylacetylene reaction (Supporting Information). After scaling, the PIE curve at *m/z* = 279 nicely matches the PIE curve of *m/z* = 278; therefore, signal at *m/z* = 279 is associated with ^{13}C-pentacene and ^{13}C-benzo[*a*]tetracene. We would like to stress that absolute photoionization cross sections of these isomers are unknown, and absolute branching ratios cannot be provided. However, the goal of the present investigation is to provide explicit evidence on the synthesis of pentacene within the 2-tetracenyl – vinylacetylene system.

With the explicit experimental evidence on the detection of pentacene ($C_{22}H_{14}$, **P1**) along with its isomer benzo[*a*]tetracene (**P2**) formed via the reaction of 2-tetracenyl with vinylacetylene in the gas phase, it is our goal to untangle the underlying reaction mechanisms. In case of complex systems, it is very beneficial to merge the experimental findings with electronic structure calculations to explore the synthetic routes (Figure 3). Our computations at the G3(MP2,CC)//B3LYP/6-311G(d,p) level of theory reveal that the 2-tetracenyl radical approaches the vinylacetylene reactant barrierlessly leading to the formation of two possible van-der-Waals complex **[i0a]** and **[i0b]** which are stabilized by 9 and 7 kJ mol^{-1} with respect to the separated reactants. The 2-tetracenyl radical adds to vinylacetylene at the terminal carbon atoms of the vinyl and ethynyl moieties yielding the intermediates [**i1]** and [**i2]**, respectively through barriers of 4 and 10 kJ mol^{-1} relative to **[i0a]** and **[i0b]**, respectively. It is important to highlight that the barrier connecting the van-der-Waals complex [**i0a**] to the resonantly stabilized free radical (RSFR) intermediate [**i1**] is *below* the energy of the separated reactants. In this sense, a barrier to addition exists, but the latter resides lower in energy than the reactants and hence is

called a *submerged barrier*.[24] Intermediate [**i1**] is central to the formation of the pentacene (**P1**) and benzo[*a*]tetracene (**P2**) products; these isomers are synthesized via the reaction sequences [**i1**] → [**i3**] → [**i4**] → [**i5**] → **P1** and [**i1**] → [**i6**] → [**i7**] → [**i8**] → **P2** involving an hydrogen atom migration from an *ortho* carbon in the attacked ring of tetracenyl to β-carbon in the side chain, cyclization, another hydrogen atom migration in the newly formed six-member ring (from the methylene moiety to the neighboring bare carbon atom), and atomic hydrogen elimination accompanied by aromatization and ring annulation. Two thermodynamically less favorable isomers, (*E*)-2-(but-1-en-3-yn-1-yl)tetracene (**P3**) and 2-(but-3-en-1-yn-1-yl)tetracene (**P4**), were not detected in our experiment. In principle, these molecules can be accessed via a hydrogen atom loss from intermediates [**i1]** and [**i2],** respectively. Considering (*E*)-2-(but-1-en-3-yn-1-yl)tetracene (**P3**), the barrier of [**i1]** → **P3** plus hydrogen is higher than the competing isomerization [**i1]** → [**i3]** and [**i1]** → **[i6]**; therefore, isomerization and eventual formation of pentacene (**P1**) and benzo[*a*]tetracene (**P2**) is preferred compared to decomposition to (*E*)-2-(but-1-en-3-yn-1-yl)tetracene (**P3**), at least at low temperatures when the entropy factor does not play a significant role. For 2-(but-3-en-1-yn-1-yl)tetracene (**P4**), the van-der-Waals complex **[i0b]** has to isomerize via a higher barrier to [**i2]** making the addition to the vinyl moiety more likely.

In conclusion, our study identified pentacene (**P1**) and benzo[*a*]tetracene (**P2**) as key products of the reaction of the 2-tetracenyl radical with vinylacetylene. The reaction was found to be barrierless and exoergic with all transition states involved located below the energy of the separated reactants. Considering these critical features along with the submerged barrier to reaction, the bimolecular reactions of the 2-tetracenyl radical with vinylacetylene reveals a facile pathway to synthesize complex PAHs – acenes - in low-temperature interstellar conditions (10 K) as present in cold molecular clouds like TMC-1 and OMC-1. Consequently, the Hydrogen-Abstraction-Vinylacetylene-Addition mechanism represents a unique low temperature pathway propelling molecular mass growth processes of aromatic systems via barrierless, successive ring annulation involving elementary reactions of aryl radical with vinylacetylene as a molecular building block.

Acknowledgments

This work was supported by the US Department of Energy, Basic Energy Sciences DE-FG02-03ER15411 (experimental studies) DE-FG02-04ER15570 (computational studies) to the University of Hawaii and Florida International University, respectively. M.A. is supported by the Director, Office of Science, Office of Basic Energy Sciences, of the U.S. Department of Energy under Contract No. DE-AC02-05CH11231, through the Gas Phase Chemical Physics program of the Chemical Sciences Division. The ALS is supported under the same contract. Ab initio calculations at Samara University were supported by the Ministry of Higher Education and Science of the Russian Federation under Grant No. 14.Y26.31.0020. H.F.B.'s group was supported by the Fonds der chemischen Industrie and Deutsche Forschungsgemeinschaft.

References

[1] S. Gabriel, E. Leupold, *Ber. Dtsch. Chem. Ges.* **1898**, *31*, 1272.

[2] E. Clar, *Ber. Dtsch. Chem. Ges. B* **1939**, *72B*, 2137.

[3] a) R. Bhatia, D. Wadhawa, G. Gurtu, J. Gaur, D. Gupta, *J. Saudi Chem. Soc.* **2019**, *23*, 925; b) Z. He, Z. Zhang, S. Bi, *J. Mater. Sci.: Mater. Electron.* **2019**, *30*, 20899.

[4] R. R. Tykwinski, *Acc. Chem. Res.* **2019**, *52*, 2056.

[5] K. Kuroda, K. Yazaki, Y. Tanaka, M. Akita, H. Sakai, T. Hasobe, N. V. Tkachenko, M. Yoshizawa, *Angew. Chem. Int. Ed.* **2019**, *58*, 1115.

[6] M. Altarawneh, I. Oluwoye, B. Z. Dlugogorski, *Combust. Flame* **2019**, *212*, 279.

[7] N. Wohner, P. Lam, K. Sattler, *Carbon* **2014**, *67*, 721.

[8] H. E. Lim, Y. Miyata, R. Kitaura, Y. Nishimura, Y. Nishimoto, S. Irle, J. H. Warner, H. Kataura, H. Shinohara, *Nat. Commun.* **2013**, *4*, 2548.

[9] A. Omont, H. F. Bettinger, C. Tönshoff, *A&A* **2019**, *625*, A41.

[10] a) L. J. Allamandola, *EAS Publ. Ser.* **2011**, *46*, 305; b) A. Tielens, L. J. Allamandola, in *Physics and Chemistry at Low Temperatures* (Ed.: Khriachtchev), Pan Stanford Publishing, **2011**, pp. 341-380; c) A. G. G. M. Tielens, *Annu. Rev. Astron. Astr.* **2008**, *46*, 289; d) A. G. G. M. Tielens, *Rev. Mod. Phys.* **2013**, *85*, 1021; e) P. J. Sarre, *J. Mol. Spectrosc.* **2006**, *238*, 1.

[11] J. Lu, D. M. Ho, N. J. Vogelaar, C. M. Kraml, R. A. Pascal, *J. Am. Chem. Soc.* **2004**, *126*, 11168.

[12] S. Yamada, K. Kinoshita, S. Iwama, T. Yamazaki, T. Kubota, T. Yajima, K. Yamamoto, S. Tahara, *Org. Biomol. Chem.* **2017**, *15*, 2522.

[13] E. Clar, J. W. Wright, *Nature* **1949**, *163*, 921.

[14] a) C. Tönshoff, H. F. Bettinger, in *Polyarenes I*, Springer, **2013**, pp. 1-30; b) K. J. Thorley, J. E. Anthony, *Isr. J. Chem.* **2014**, *54*, 642; c) J. E. Anthony, *Angew. Chem. Int. Ed.* **2008**, *47*, 452; d) J. E. Anthony, *Chem. Rev.* **2006**, *106*, 5028.

[15] M. Suzuki, T. Aotake, Y. Yamaguchi, N. Noguchi, H. Nakano, K.-i. Nakayama, H. Yamada, *J. Photochem. Photobiol., C* **2014**, *18*, 50.

[16] a) M. Watanabe, K.-Y. Chen, Y. J. Chang, T. J. Chow, *Acc. Chem. Res.* **2013**, *46*, 1606; b) M. Watanabe, et al., *Nat. Chem.* **2012**, *4*, 574.

[17] a) R. Einholz, T. Fang, R. Berger, P. Grüninger, A. Früh, T. Chassé, R. F. Fink, H. F. Bettinger, *J. Am. Chem. Soc.* **2017**, *139*, 4435; b) C. Tönshoff, H. F. Bettinger, *Angew. Chem. Int. Ed.* **2010**, *49*, 4125; c) B. Shen, J. Tatchen, E. Sanchez-Garcia, H. F. Bettinger, *Angew. Chem. Int. Ed.* **2018**, *57*, 10506; *Angew. Chem.* **2018**, *130*, 10666.

[18] a) J. Krüger, et al., *Angew. Chem. Int. Ed.* **2017**, *56*, 11945; *Angew. Chem.* **2017**, *129*, 12107; b) J. Krüger, et al., *ACS nano* **2018**, *12*, 8506; c) R. Zuzak, R. Dorel, M. Kolmer, M. Szymonski, S. Godlewski, A. M. Echavarren, *Angew. Chem. Int. Ed.* **2018**, *57*, 10500; *Angew. Chem.* **2018**, *130*, 10660.

[19] A. M. Mastral, M. S. Callen, *Environ. Sci. Technol.* **2000**, *34*, 3051.

[20] B. Wen, K. K. Wang, *Pure Appl. Chem.* **2012**, *84*, 893.

[21] P. Makos, A. Przyjazny, G. Boczkaj, *J. Chromatogr. A* **2018**, *1570*, 28.

[22] F. Zhang, Y. S. Kim, R. I. Kaiser, S. P. Krishtal, A. M. Mebel, *J. Phys. Chem. A* **2009**, *113*, 11167.

[23] D. Stahl, F. Maquin, *Chem. Phys. Lett.* **1984**, *108*, 613.

[24] L. Zhao, R. I. Kaiser, B. Xu, U. Ablikim, M. Ahmed, M. M. Evseev, E. K. Bashkirov, V. N. Azyazov, A. M. Mebel, *Angew. Chem. Int. Ed.* **2020**, *59*, 4051.

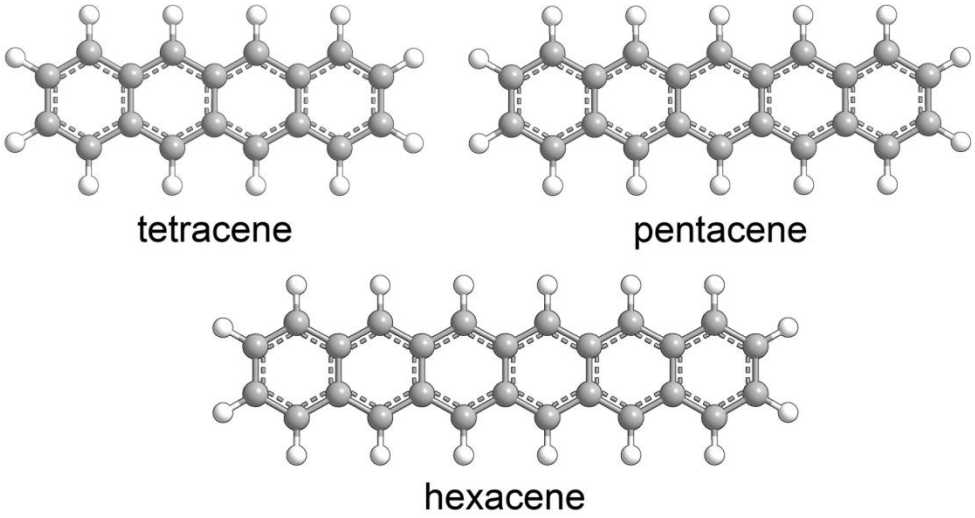

Scheme 1. Molecular structures of the three simplest acenes: tetracene ($C_{18}H_{12}$), pentacene ($C_{22}H_{14}$), and hexacene ($C_{26}H_{16}$). Carbon and hydrogen atoms are color coded in gray and white, respectively.

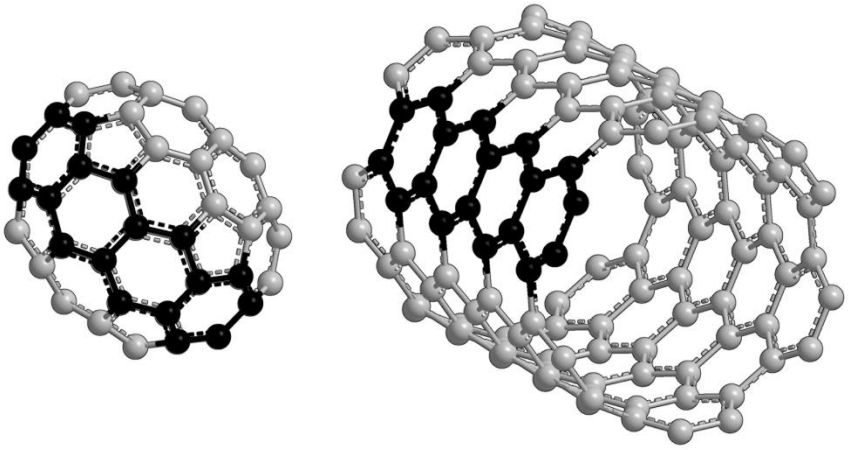

Scheme 2. Acenes as fundamental building blocks in fullerenes and carbon nanotubes; the acene moiety is highlighted in black.

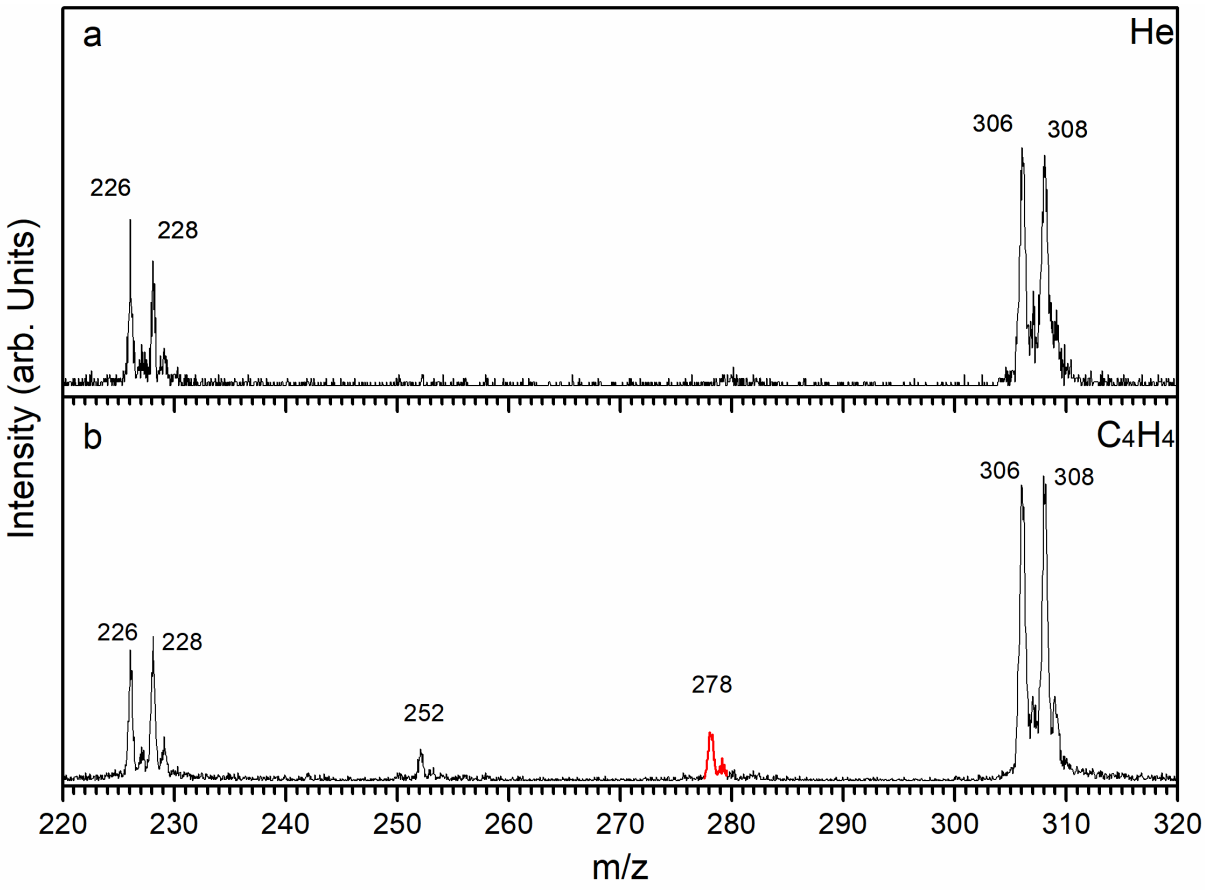

Figure 1. Photoionization mass spectra recorded at a photoionization energy of 9.0 eV. (a) 2-tetracenyl ($C_{18}H_{11}^{\bullet}$) - helium (He) system; (b) 2-tetracenyl ($C_{18}H_{11}^{\bullet}$) - vinylacetylene (C_4H_4) system. The mass peaks of the newly formed $C_{22}H_{14}$ (*m/z* = 278) species along with the ^{13}C-substituted counterpart (*m/z* = 279) are highlighted in red.

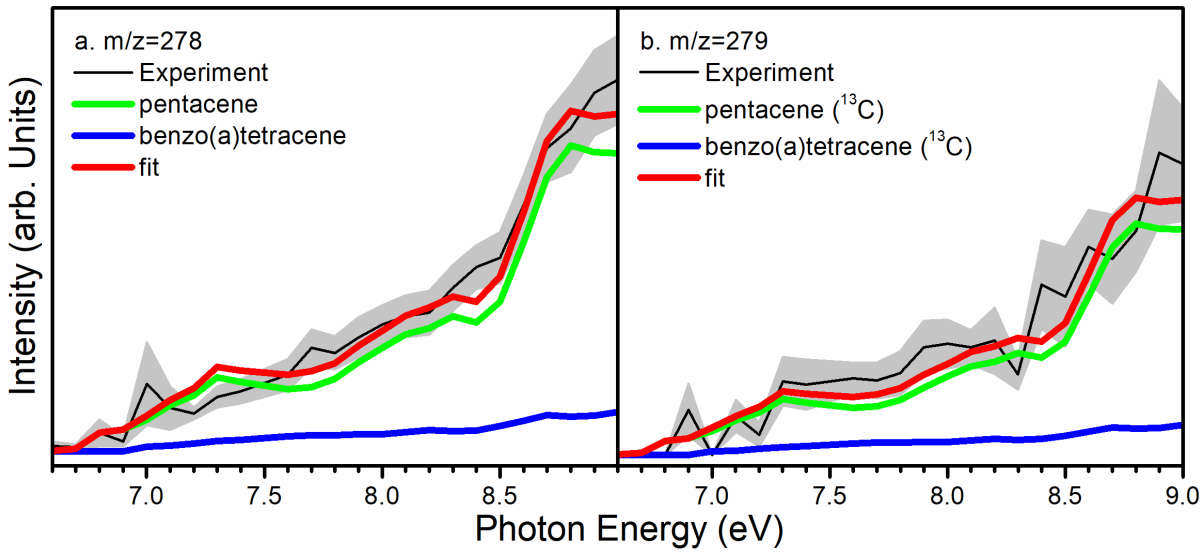

Figure 2. Photoionization efficiency (PIE) curves for *m/z* = 278 and 279. Black: experimentally derived PIE curves with the error area presented in gray; green: pentacene reference PIE curve; blue: benzo[*a*]tetracene PIE curve; red: overall fit. The overall error bars consist of two parts: ±10% based on the accuracy of the photodiode and a 1 σ error of the PIE curve averaged over the individual scans.

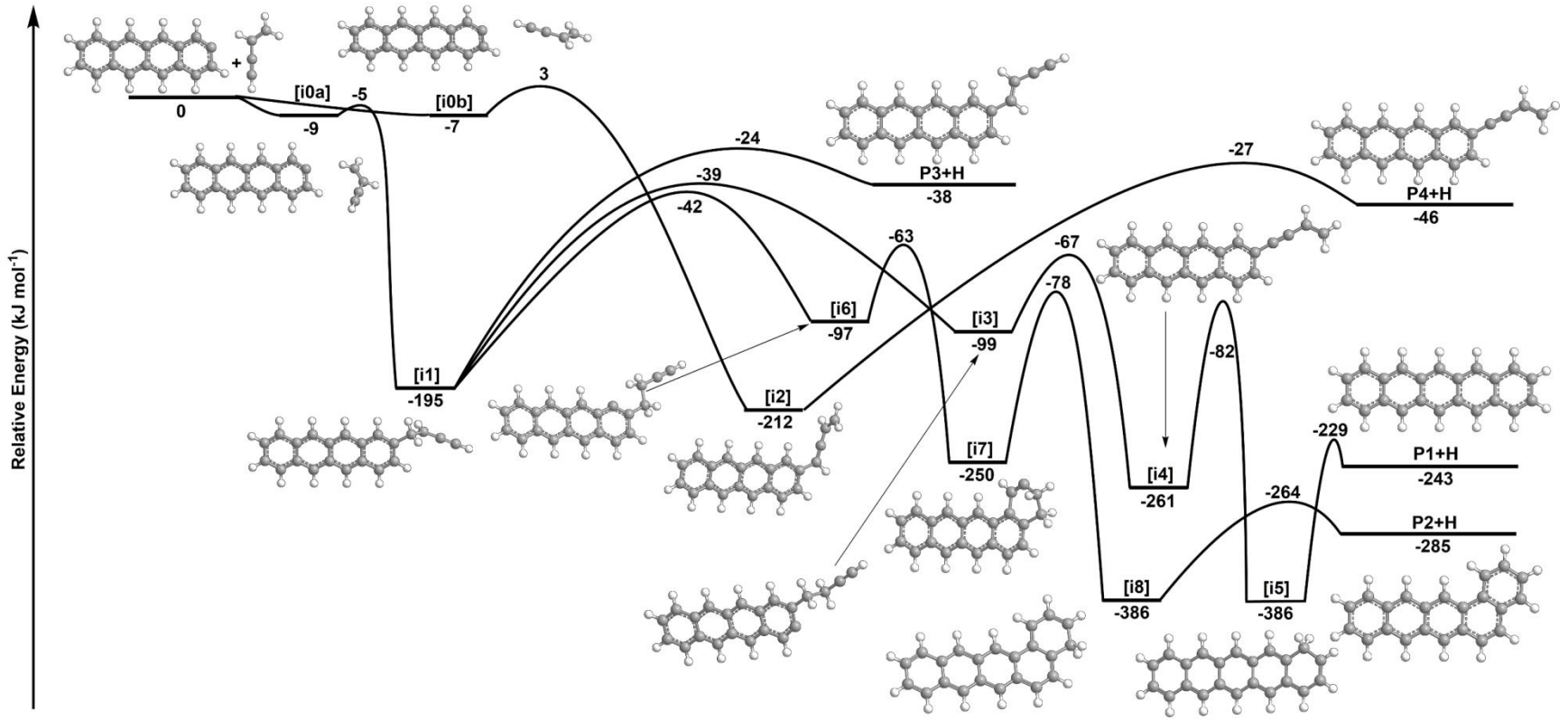

Figure 3. Potential energy surface (PES) for the 2-tetracenyl ($C_{18}H_{11}^{\bullet}$) reaction with vinylacetylene (C_4H_4). This PES was calculated at the G3(MP2,CC)//B3LYP/6-311G(d,p) level of theory leading to pentacene and its isomer benzo[*a*]tetracene. The relative energies are given in kJ mol^{-1}.

Supporting Information

A Free Radical Prompted Barrierless Gas Phase Synthesis of Pentacene

Long Zhao, Ralf I. Kaiser*

Department of Chemistry, University of Hawaii at Manoa, Honolulu, HI, 96822, USA

Wenchao Lu, Musahid Ahmed*

Chemical Sciences Division, Lawrence Berkeley National Laboratory, Berkeley, CA 94720, USA

Mikhail M. Evseev, Eugene K. Bashkirov

Samara National Research University, Samara 443086, Russian Federation

V. N. Azyazov

Lebedev Physical Institute, Samara 443011
and Samara National Research University, Samara 443086, Russian Federation

Alexander M. Mebel*

Department of Chemistry and Biochemistry, Florida International University, Miami, FL 33199, USA

Christina Tönshoff, Florian Reicherter, Holger F. Bettinger*

Institute of Organic Chemistry, University of Tübingen, Auf der Morgenstelle 18; 72076 Tübingen, Germany

* Corresponding authors:
Prof. Dr. Ralf I. Kaiser <ralfk@hawaii.edu>
Dr. Musahid Ahmed <MAhmed@lbl.gov>
Prof. Dr. Alexander M. Mebel <mebela@fiu.edu>
Prof. Dr. Holger F. Bettinger <holger.bettinger@uni-tuebingen.de>

Methods

Experimental: The experimental studies were conducted at the Advanced Light Source (ALS) at the Chemical Dynamics Beamline (9.0.2.) exploiting a high-temperature chemical reactor;[1] this unit comprises of a resistively-heated silicon carbide (SiC) tube of 20 mm length and 1 mm inner diameter and is incorporated within the source chamber of the molecular beam apparatus operated with a Wiley-McLaren reflectron time-of-flight mass spectrometer (Re-TOFMS). Here, 2-tetracenyl radicals ($C_{18}H_{11}^{\bullet}$) were produced at concentrations of less than 0.1% *in situ* via pyrolysis of the 2-bromotetracene precursor ($C_{18}H_{11}Br$) seeded in vinylacetylene/helium (5% C_4H_4; 95 % He; Applied Gas) carrier gas at a pressure of 300 Torr. Due to the low vapor pressure of the precursor, 2-bromotetracene was placed inside the nozzle assembly and heated to 613 ± 10 K operated with an aperture of 0.2 mm. The temperature of the SiC tube was monitored using a Type-C thermocouple and was maintained at 1,500 ± 10 K. At this temperature, 2-bromotetracene dissociates to the 2-tetracenyl radical plus atomic bromine *in situ* followed by the reaction of the aromatic radical with vinylacetylene. All reaction products were expanded supersonically and passed through a 2 mm diameter skimmer located 10 mm downstream the reactor; the products then entered the main chamber and were photoionized in the extraction region of the mass spectrometer by exploiting quasi-continuous tunable synchrotron vacuum ultraviolet (VUV) light. The ions formed via soft photoionization are extracted and introduced onto a microchannel plate detector through an ion lens. Photoionization efficiency (PIE) curves, which report ion counts as a function of photon energy from 6.60 eV to 9.00 eV with a step interval of 0.05 eV at a well-defined mass-to-charge ratio (*m/z*), were produced by integrating the signal collected at the specific *m/z* for the species of interest and normalized to the photon flux; the repeller plate of the ReTOF was pulsed at a voltage of 1200 V with a pulse duration of 2.5 μs; the multichannel plate was held at 4450 V. An ionization efficiency curve produced by photoionization is comparable to a first derivative of its electron-ionization counterpart.[2] The residence time in the reactor tube under our experimental condition are few hundreds of μs.[3] The control experiment was carried out by expanding neat helium carrier gas with the 2-bromotetracene precursor into the resistively-heated SiC tube. Calibration experiments of the PIE curves of pentacene and benzo[*a*]tetracene were conducted in the same experimental setup by seeding these molecules in neat helium carrier gas. 2-Bromotetracene and benzo[*a*]tetracene were synthesized as described in the Supporting Information; pentacene (99.999 %) was acquired from TCI America.

Theoretical Calculation: The energies and molecular parameters of the local minima and transition states involved in the reaction were computed at the G3(MP2,CC)//B3LYP/6-311G(d,p) level of theory with a chemical accuracy of at least 8 kJ mol^{-1} for the relative energies and 0.01–0.02 Å for bond lengths as well as 1–2° for bond angles.[4] Within this theoretical scheme, geometries are optimized and vibrational frequencies are computed using the density functional B3LYP/6-311G(d,p) method and single-point energies are refined as:

E[G3(MP2,CC)] = E[CCSD(T)/6-311G(d,p)] + E[MP2/G3Large)] – E[MP2/6-311G(d,p)] + ZPE[B3LYP/6-311G(d,p)]

The GAUSSIAN 09[5] and MOLPRO 2010 program packages[6] were exploited for the *ab initio* calculations.

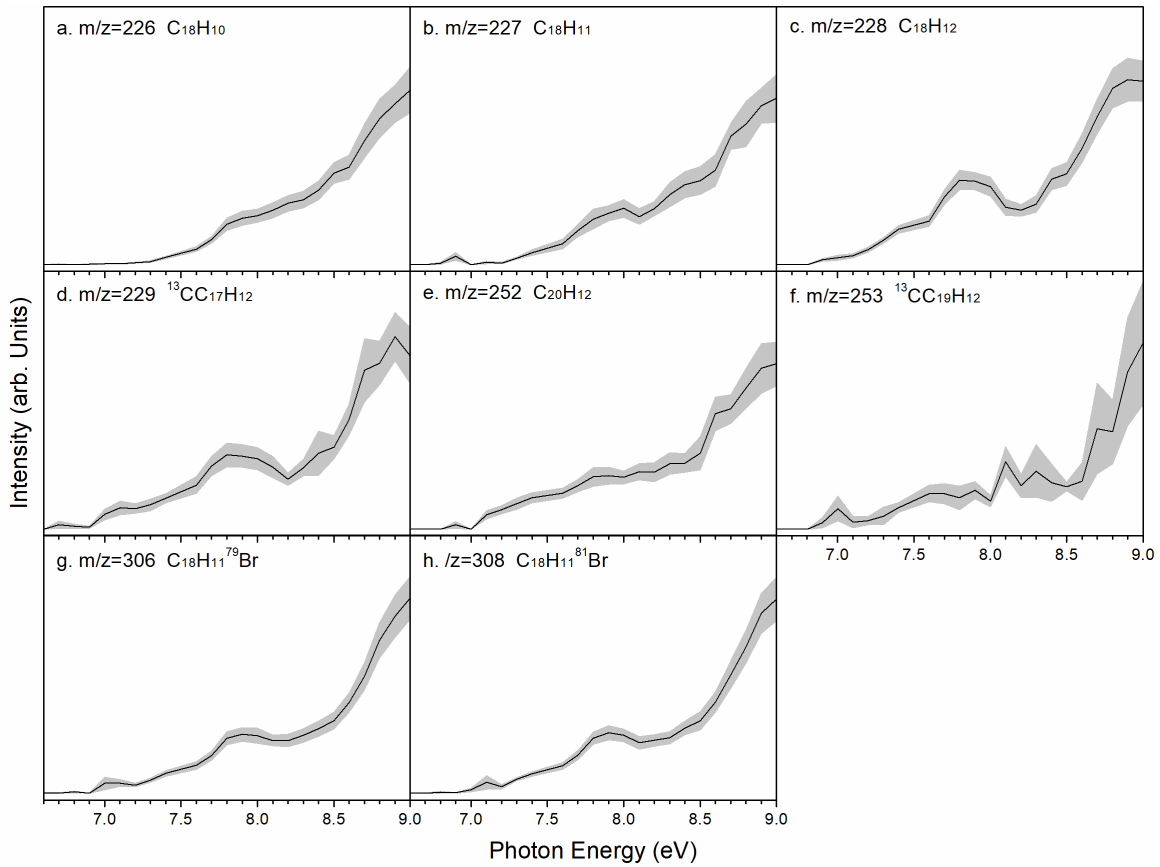

Figure S1. Photoionization efficiency (PIE) curves of distinct ions detected in 2-bromotetracene - vinylacetylene system.

Signal at m/z = 252 and 253 can be associated with $C_{20}H_{12}$ molecule(s) which originate from the reaction of 2-tetracenyl with acetylene, with the latter representing a minor impurity from the vinylacetylene reactant.[7] After scaling, the graphs of *m/z* = 252 and 253 overlap below 8.6 eV indicating that the signal at *m/z* = 253 can be attributed to the ^{13}C-counterpart of *m/z* = 252. Due to the lack of calibrated PIE curves, we could not identify the products at *m/z* = 252 ($C_{20}H_{12}$) and 253 with m/z = 252 attributed to dissociative photoionization of the precursor molecule. Signal at *m/z* = 227 can be connected to the 2-tetracenyl radical. *m/z* = 226 and *m/z* = 228 originate from the hydrogen atom loss from and hydrogen atom addition to 2-tetracenyl leading to tetracyne isomers and tetracene, respectively; signal at *m/z* = 228 can also originate from dissociative photoionization of the precursor. Signals at *m/z* = 306 and 308 are attributed to the precursor 2-bromotetracene ($C_{18}H_{11}{}^{79}Br$ and $C_{18}H_{11}{}^{81}Br$).

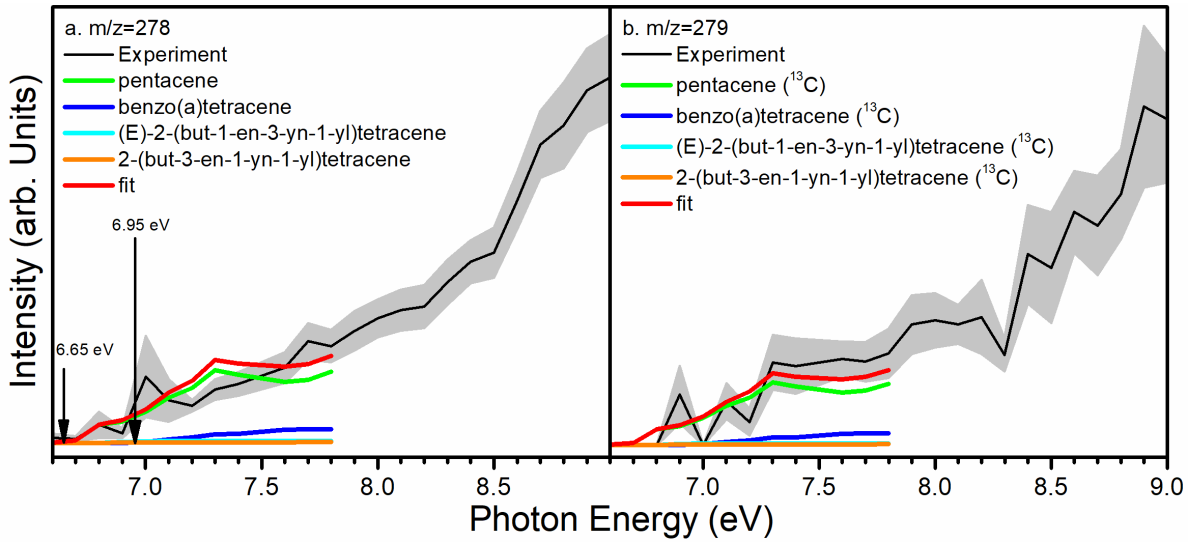

Figure S2. Photoionization efficiency (PIE) curves for *m/z* = 278 and 279. Black: experimentally derived PIE curves with the error bars presented in gray; green: pentacene reference PIE curve; blue: benzo[*a*]tetracene PIE curve; cyan: (*E*)-2-(but-1-en-3-yn-1-yl)tetracene; orange: 2-(but-3-en-1-yl)tetracene; red: overall fit. The overall error limits consist of two parts: ± 10 % based on the accuracy of the photodiode and a 1 σ error of the PIE curve averaged over the individual scans.

To this fit, we added the PIE curves for (*E*)-2-(but-1-en-3-yn-1-yl)tetracene and 2-(but-3-en-1-yl)tetracene computed at the G3(MP2,CC)//B3LYP/6-311G(d,p) level of theory; the branching ratios contributing to the overall intensity is only 2 ± 2 % and 1 ± 1%, respectively. Thus, even these two isomers can be produced in the experiment, the amount would be very limited and negligible; note that the experimental data can be fit within the error limits without any contribution of both isomers. As a conclusion, it is vital to highlight that the PIE curves of the $C_{22}H_{14}$ isomers are *discretely connected* to the specific isomers emphasizing that the co-existence of additional isomers in the molecular beam besides pentacene and benzo[*a*]tetracene such as (*E*)-2-(but-1-en-3-yn-1-yl)tetracene and 2-(but-3-en-1-yn-1-yl)tetracene can be excluded since their presence would change the shape of the PIE curve. Therefore, our data analysis reveals that only pentacene and benzo[*a*]tetracene contribute to signal at *m/z* = 278 within our error limits. These errors are connected to the 1 σ error of the PIE curve averaged over multiple scans and the ± 10 % error stated by the manufacturer as the accuracy of the photodiode.

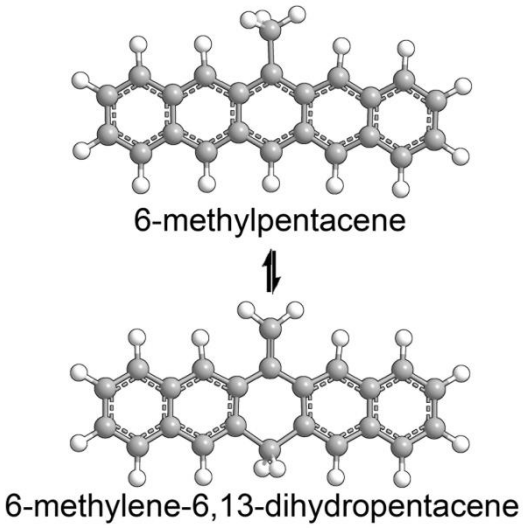

Scheme S1. Tautomeric equilibrium between 6-methylene-6,13-dihydropentacene and 6-methyl-pentacene.

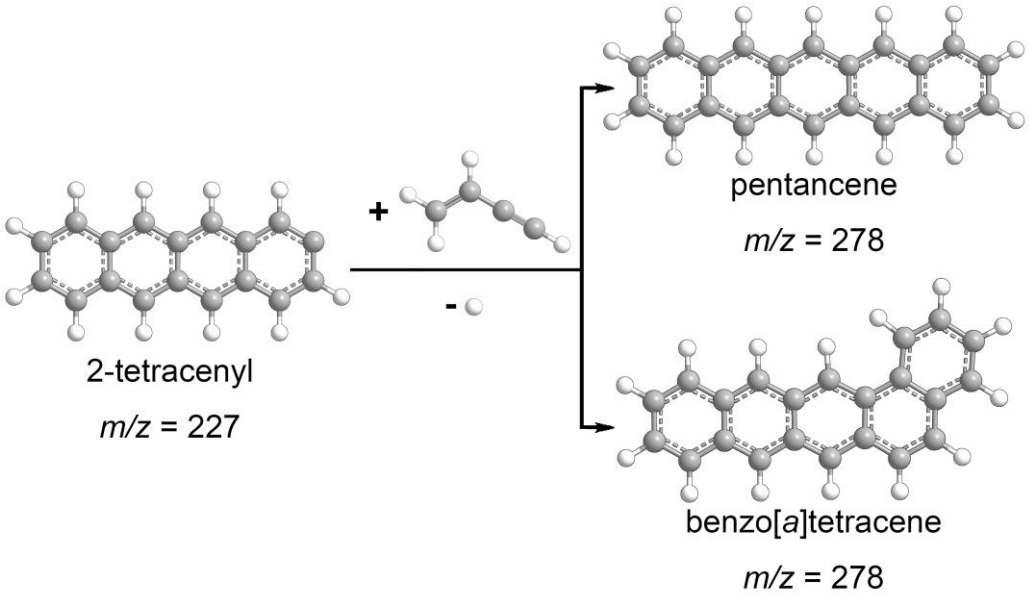

Scheme S2. Schematic representation on the formation of pentacene and its benzo[*a*]tetracene isomer through the reaction of the 2-tetracenyl radical ($C_{18}H_{11}$) with vinylacetylene (C_4H_4).

Synthesis method

General Information

All commercially available reagents were used without further purification.

NMR spectra were recorded on Bruker AVANCE III HD 400 MHz and Bruker AVIII HDX+700 spectrometers. Spectra were recorded in $CDCl_3$ or $CDCl_3/CS_2$ (99.9% extra pure, AcrosOrganics) as indicated and chemical shifts were referenced to the residual solvent peak.

Mass spectra (EI) were obtained from a Finnigan TSQ 70 with quadrupole analyzer, and high-resolution data were obtained using a Finnigan MAT 95 spectrometer with sector field analyzer.

Absorption spectra were measured on a PerkinElmer LAMDA 1050 spectrometer.

Synthesis of 2-Bromotetracene[8]

2-Bromotetracene is obtained by a reaction sequence similar to that described by Kitamura et al.[8a] with the difference that in the last step instead of a Meerwein-Ponndorf reaction a reduction with $NaBH_4$ in iPrOH was performed.[9]

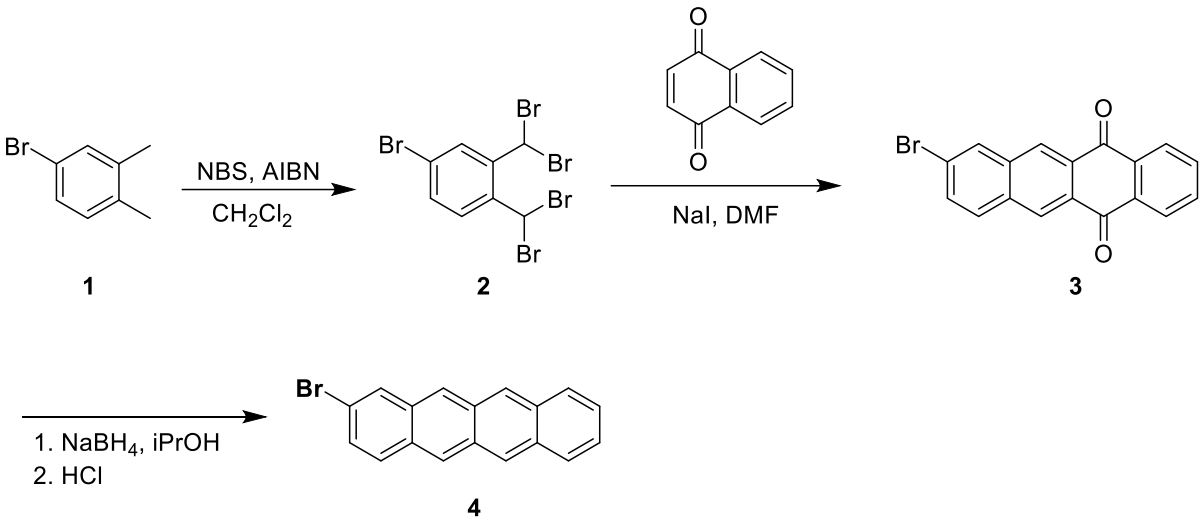

Compound 2 was synthesized by Wohl-Ziegler bromination according to the literature,[10] but CH_2Cl_2 was used as solvent instead of CCl_4. **2** was obtained together with the threefold benzylic brominated compounds. After column chromatopraphy, **2** is obtained together with mixed fractions containing **2** and threefold brominated compounds, which can also be used in the subsequent Diels-Alder reaction.

9.6 g N-Bromosuccinimid NBS (54.04 mmol) were suspended in 50 ml of CH_2Cl_2 and 3.65 ml (5g, 27.07 mmol) 4-bromo-o-xylol **1** and 0.15 g azobis(isobutyronitrile) AIBN (0.88 mmol)

were added. The mixture was refluxed for 72 h and after 24h and 48h another 9.6 g NBS and 0.15 g AIBN were added. After cooling the mixture was filtered, the solid was washed with CH_2Cl_2 and the combined filtrate and washing solution were washed three times with water, aqueous $Na_2S_2O_3$ and brine. After drying over $MgSO_4$ the solvent was evaporated and the residue was purified by column chromatography (silica; hexane). 4.65 g (9.4 mmol, 34.7 %) of **2** were obtained together with 7.7g of a mixed fraction containing **2** and threefold brominated compounds. The mixed fraction can also be used in the Diels-Alder reaction in the next step. NMR data of **2**:

^{1}H (400MHz, $CDCl_3$): 7.81 (s, 1H), 7.58-7.48 (m, 2H), 7.04(m, 2H) ppm

^{13}C (100 MHz, $CDCl_3$): 139.04 (broad), 136.60 (broad), 133.50, 132.14 (broad), 131.08 (broad), 124.12, 35.25, 34.81 ppm

Compound 3[8a]

Under N_2 3.94 g (26.28 mmol) NaI and 1.00 g (6.31 mmol) of 1,4-naphthoquinone were suspended in 30 ml DMF and 3.29 g (6.57 mmol) **2** were added. The mixture was heated to 110 °C for 48 h and after cooling the precipitated solid was isolated by filtration, washed with water, methanol and acetone, and dried under vacuum. 1.68 g (4.98 mmol, 78 %) of **3** were obtained as gold-yellow solid.

^{1}H (400MHz, $CDCl_3$): 8.84 (s, 1H), 8.77 (s, 1H), 8.42-8.39 (m, 2H), 8.28 (m, 1H), 7.98 (d, 1H), 7.86-7.83 (m, 2H), 7.79-7.76 (dd, 1H) ppm

^{1}H (400MHz, D_2SO_4): 9.05 (s, 1H), 8.84 (s, 1H), 8.48-8.42 (m, 2H), 8.28 (s, 1H), 8.13-8.06 (m, 2H), 8.00-7.98 (m, 1H), 7.94-7.92 (m, 1H)

^{13}C (100MHz, D_2SO_4): 187.74, 186.79, 141.34, 140.15, 138.26, 137.59, 137.40, 135.09, 134.40, 134.32, 132.42, 132.38, 132.24, 132.18, 130.83, 126.12, 124.11

Compound 4[8]

0.2 g (0.59 mmol) **3** and 0.31 g $NaBH_4$ (8 mmol) in 20 ml of *i*-PrOH were heated under reflux for 24 h in the dark. After cooling 20 ml of 2M HCl were added dropwise and the mixture was refluxed for 3 h. After cooling the obtained orange solid was washed with water, methanol, acetone and hexane. Then the solid was suspended in acetone, sonicated for a few minutes, centrifuged and the solvent removed. This was repeated three more times with fresh acetone and then four times using $CHCl_3$ as solvent. 0.14 g (0.46 mmol) of **4** was obtained (77%). **4** is hardly soluble in common organic solvents.

^{1}H (400MHz, CS_2/$CDCl_3$): 8.60 (s, 3H), 8.53 (s, 1H), 8.13 (s, 1H), 7.96-7.95 (m, 2H), 7.86 (d, 1H), 7.41-7.38 (m, 3H)

MS (EI, 70 eV, m/z (%)): 308/306 ($M^{+\cdot}$,100), 226 ($M^{+\cdot}$-Br), 113

HR-MS: *m/z*: calcd for $C_{18}H_{11}Br$ 306.003864; found 306.00053

UV/Vis ($CHCl_3$): λ_{max} = 284, 299, 378, 400, 421, 448, 478 nm (due to the low solubility no extinction coefficients could be determined)

Synthesis of Benzo[a]tetracene

1,2-Benzotetracene is a known compound.[11] It was synthesized in a reaction sequence similar to the one used for 2-bromotetracene. The final reduction with $NaBH_4$ had to be done in two separated steps, but the intermediate hydroquinone was not purified as described in the literature for the synthesis of 2,3-dibromotetracene.[9b]

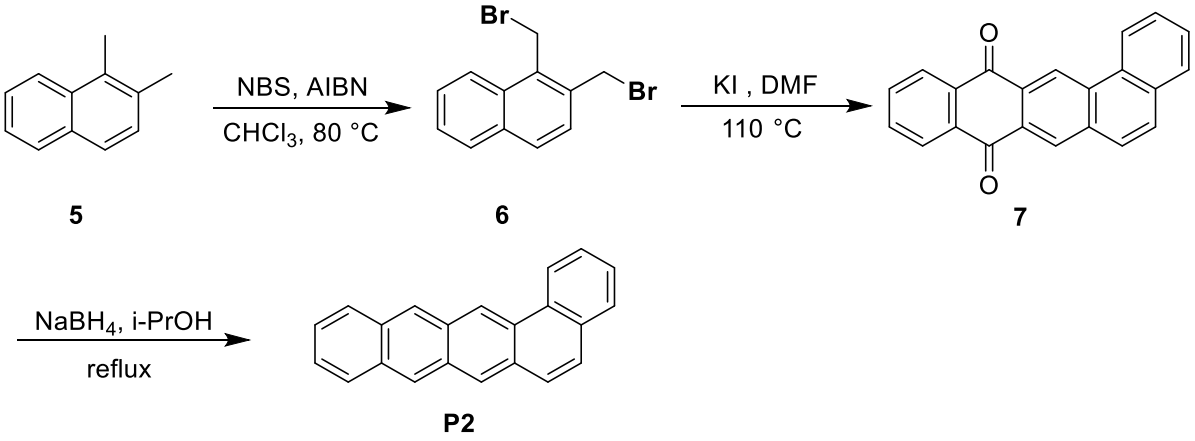

Comound 6 was prepared by Wohl-Ziegler bromination of **5** according to García et al.[12]

Compound 7[13]

Under N_2 1.5 g (4.8 mmol) of **6**, 0.52 g (3.3 mmol) 1,4-naphthoquinone and 5.2 g (31.2 mmol) KI were stirred at 110 °C for 24 h. After cooling to RT the solid was isolated by filtration and washed with water, acetone, and CH_2Cl_2 and dried under vacuum. **7** was obtained as a yellow solid in 51 % yield (0.52g, 1.7 mmol).

^{1}H (700 MHz, $CDCl_3$): 9.65 (s, 1H), 8.92 (d, 1H), 8.84 (s, 1H), 8.44-8.39 (m, 2H), 7.97-7.94 (m, 3H), 7.86-7.78 (m, 3H), 7.75-7.71 (m, 1H)

^{13}C (176 MHz, $CDCl_3$): 183.15, 183.05, 135.05, 134.37, 134.28, 134.16, 134.14, 133.62, 133.08, 130.82, 130.51, 130.50, 130.28, 128.96, 128.55, 127.89, 127.48, 127.39, 127.19, 123.92, 123.44

MS (EI, 70 eV, m/z (%)): 308.2 (100, $M^{+\cdot}$), 280.1 (28), 252.1 (39)

HR-MS: *m/z*: calcd for $C_{22}H_{12}O_2$ 308.083181; found 308.08373

Compound P2 was prepared as described in the literature for 2,3-dibromotetracene.[9b]

0.5 g (1.62 mmol) of **7** and 3.52 g (93 mmol) $NaBH_4$ were dissolved in 150 ml of *i*-PrOH under N_2 and stirred for 2 h at RT and then for 12 h under reflux. After cooling 6M HCl was added until no more gas evolved and then it was refluxed for 4 h. After cooling the precipitated solid was separated by filtration. This solid was again dissolved in 100 ml *i*-PrOH under N_2 and 2.5 g (66 mmol) were added and the mixture refluxed for 40 h. After cooling it was quenched with 3 M HCl and refluxed again for 2 h. After cooling the solid was separated by filtration and washed with water, acetone and hexane. The solid was put in 100 ml toluene and kept overnight at -18 °C and the bright yellow solid was isolated in 85 % yield (0.39 g; 1.4 mmol).

^{1}H (700MHz, $CDCl_3/CS_2$): 9.26 (s, 1H), 8.76 (d, 1H), 8.69 (s, 1H), 8.60 (s, 1H), 8.47 (s, 1H), 8.02-8.00 (m, 2H), 7.73-7.70 (d(1H) + d(1H)), 7.65-7.63 (m, 1H), 7.59-7.55 (m, 1H), 7.50 (d, 1H), 7.46-7.42 (m, 2H)

^{13}C (176MHz, $CDCl_3/CS_2$): 131.76, 131.49, 131.43, 130.46, 130.42, 130.14, 128.58, 128.44, 128.11, 128.05, 127.44, 127.16, 127.09, 126.81, 126.72, 126.58, 125.85, 125.16, 125.10, 122.77, 121.57

MS (EI, 70 eV, m/z (%)): 278.1 (100, $M^{+\cdot}$), 139 (22)

HR-MS: *m/z*: calcd for $C_{22}H_{14}$ 278.109001; found 278.1080

UV-vis ($CHCl_3$) λ_{max} (ε): 294 (383010), 305 (58300), 318 (50700), 362 (1300), 381 (2100), 402 (3500), 425 (5400), 453(5200)

NMR Spectra

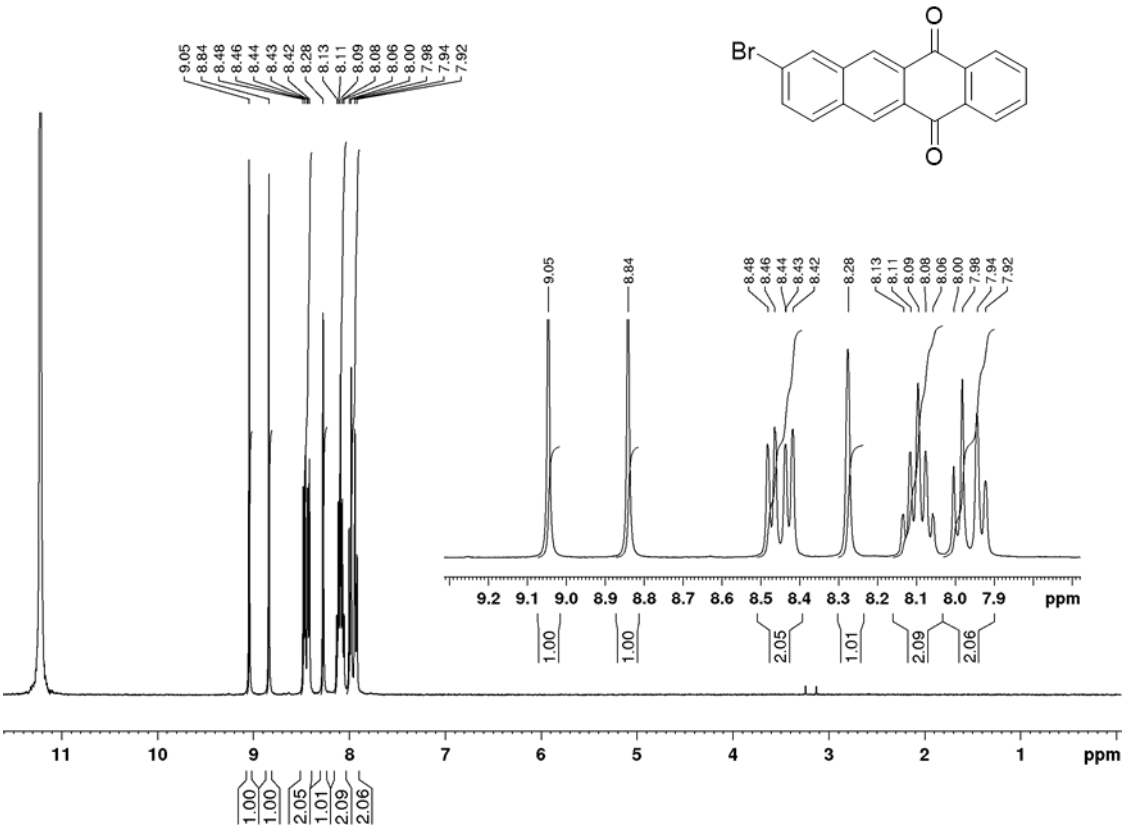

Figure S3: ^{1}H NMR spectrum of 8-bromotetracene-5,12-dione (compound **3**) in D_2SO_4.

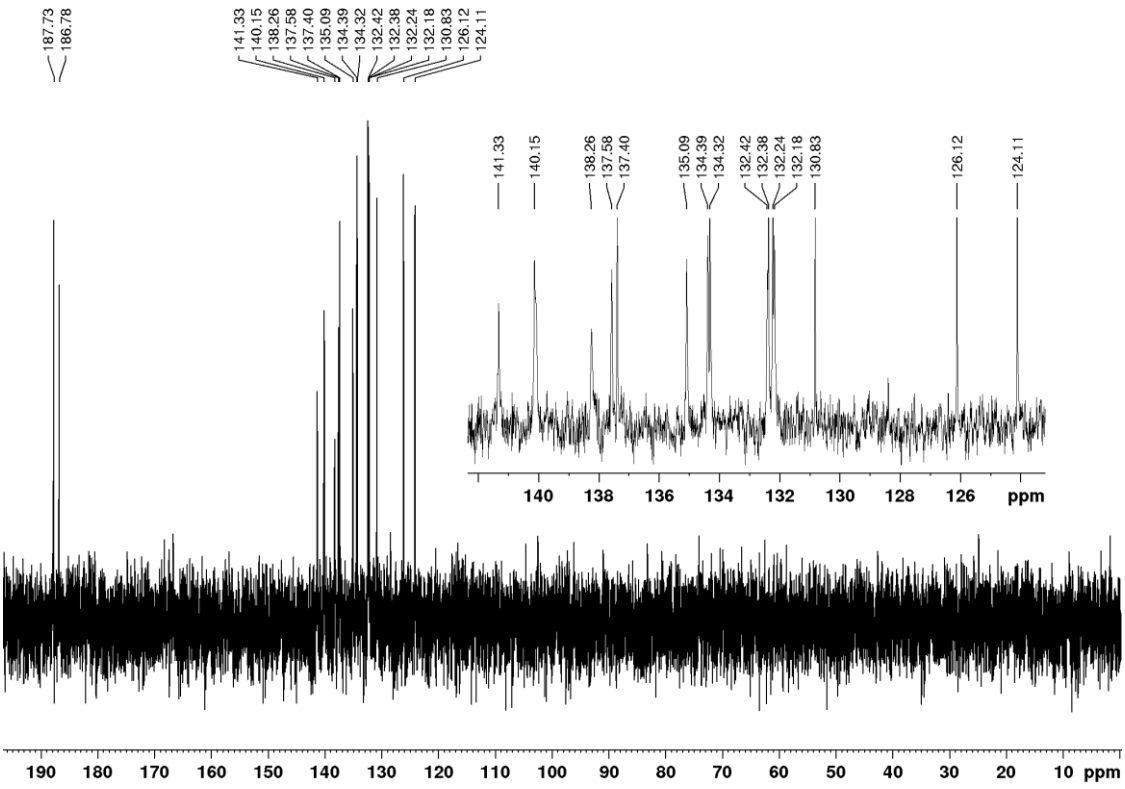

Figure S4: ^{13}C NMR spectrum of 8-bromotetracene-5,12-dione (compound **3**) in D_2SO_4.

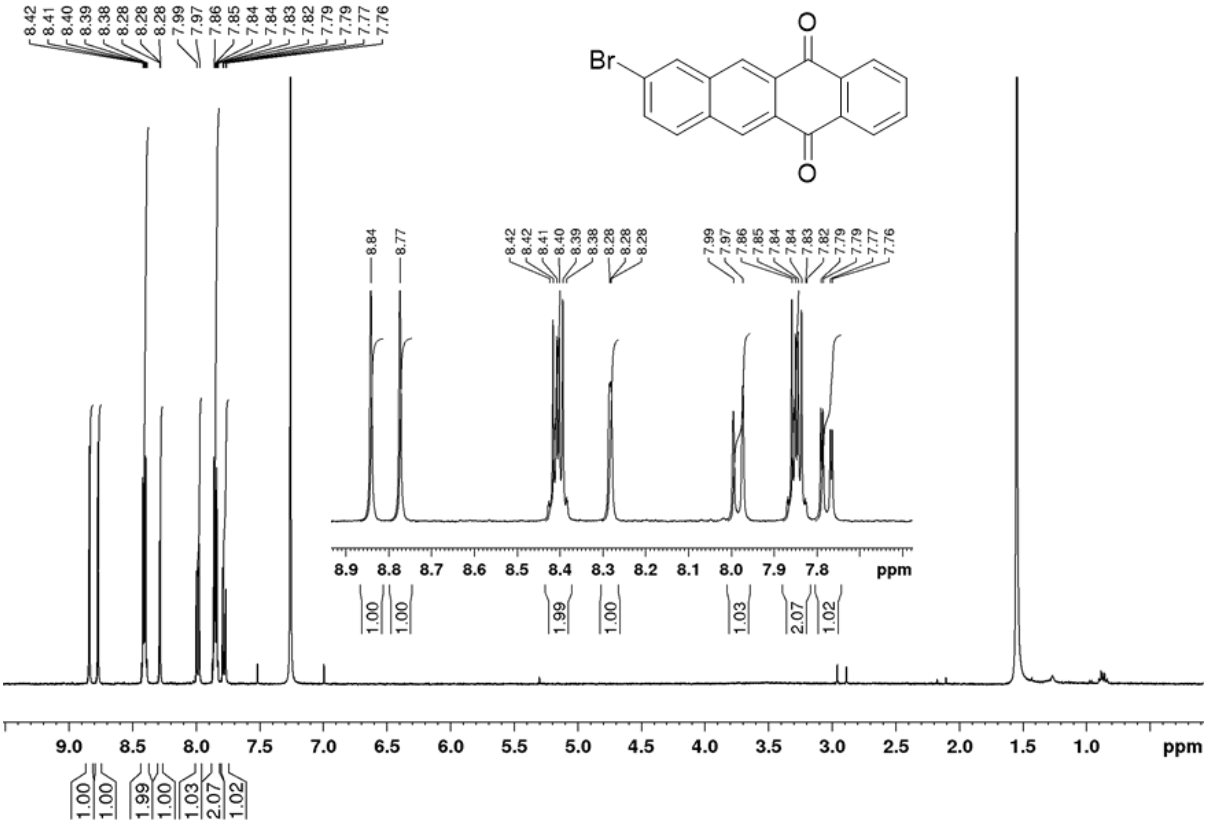

Figure S5: ^{1}H NMR spectrum of 8-bromotetracene-5,12-dione (compound **3**) in $CDCl_3$.

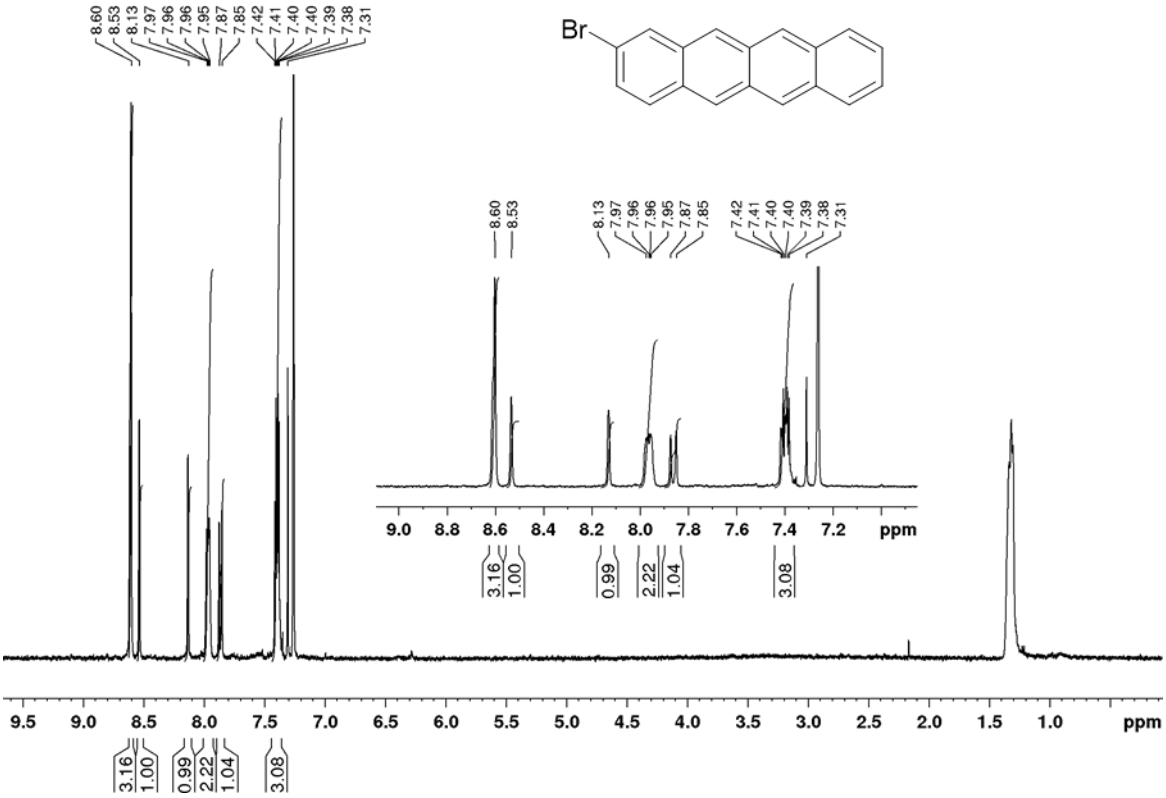

Figure S6: ^{1}H NMR spectrum of 2-bromotetracene (compound **4**) in $CDCl_3/CS_2$; the peak at 7.31 ppm is due to an impurity in the CS_2.

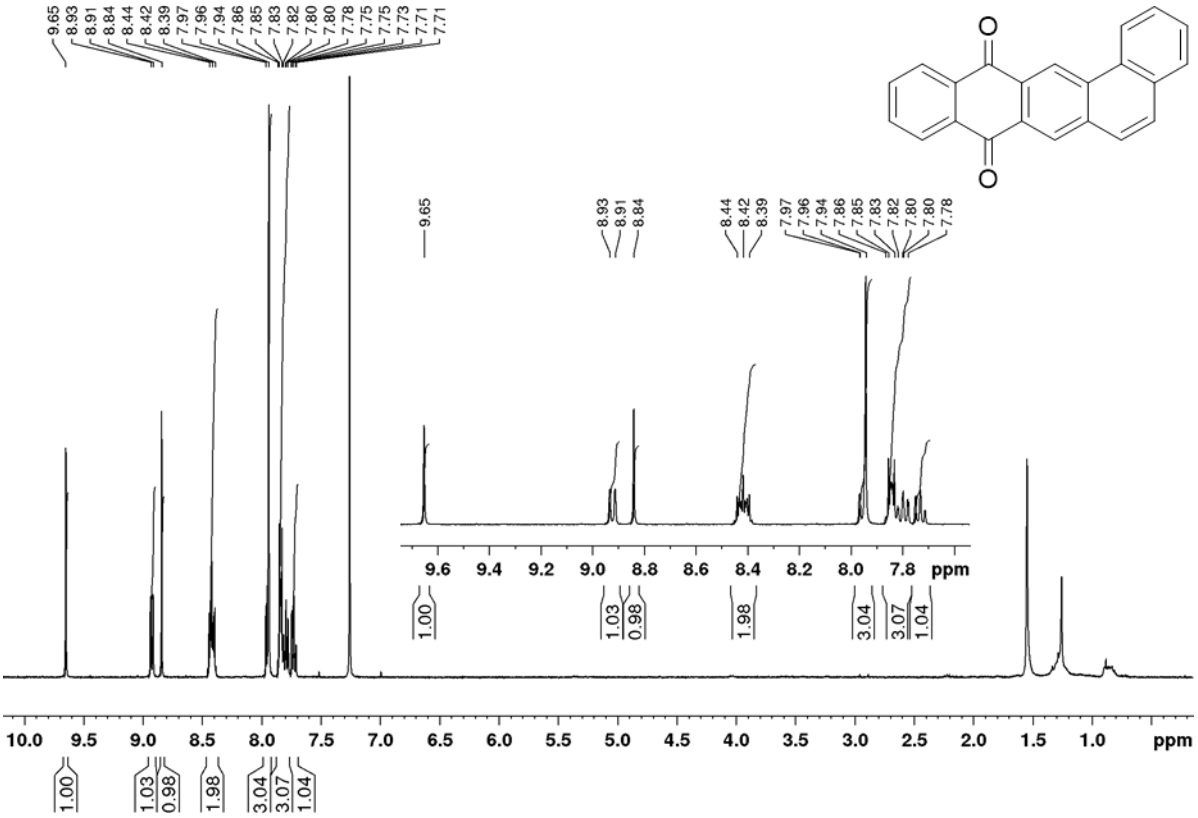

Figure S7: ^{1}H NMR spectrum of benzo[*a*]tetracene-8,13-dione (compound **7**) in $CDCl_3$.

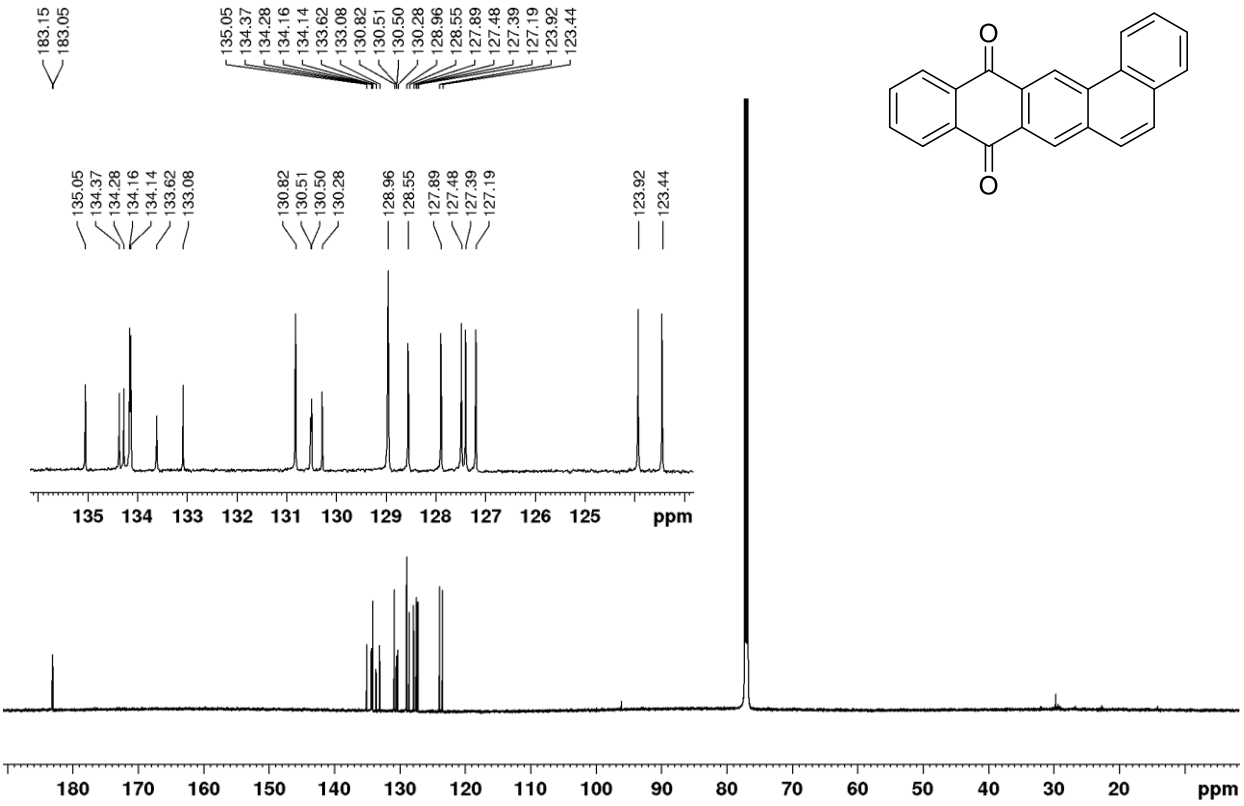

Figure S8: ^{13}C NMR spectrum of benzo[*a*]tetracene-8,13-dione (compound **7**) in $CDCl_3$.

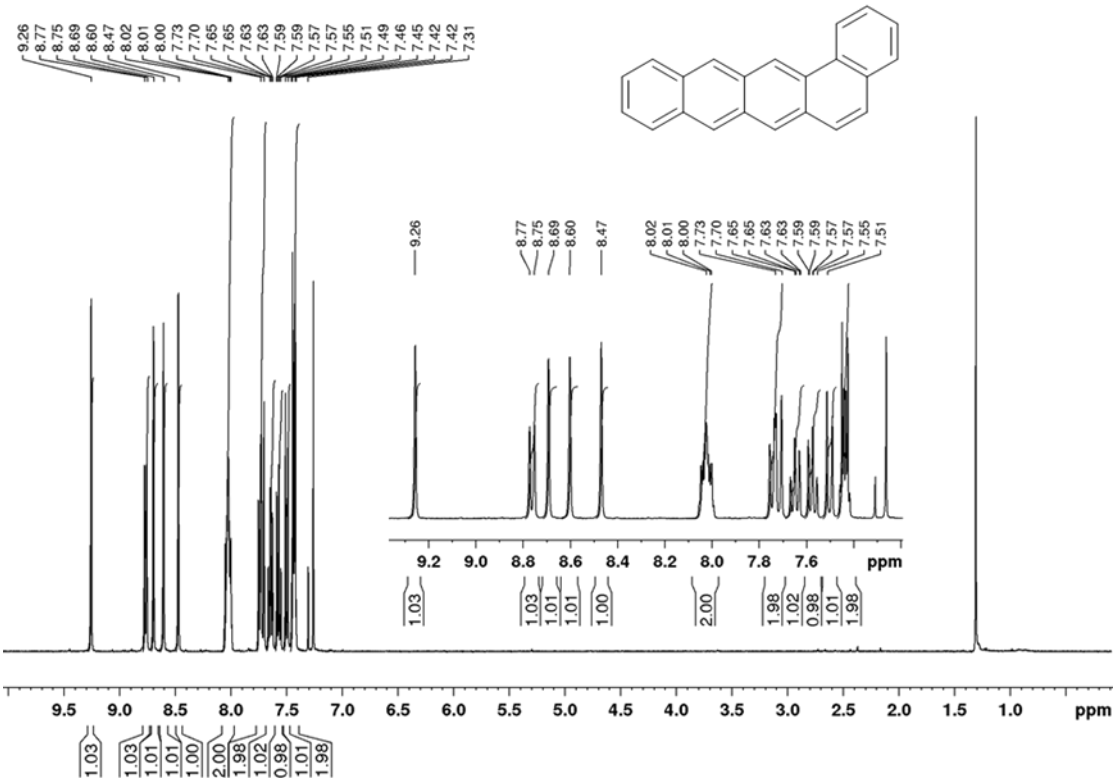

Figure S9: ^{1}H NMR spectrum of benzo[*a*]tetracene (compound **P2**) in $CDCl_3/CS_2$; the peak at 7.31 ppm is due to an impurity in CS_2.

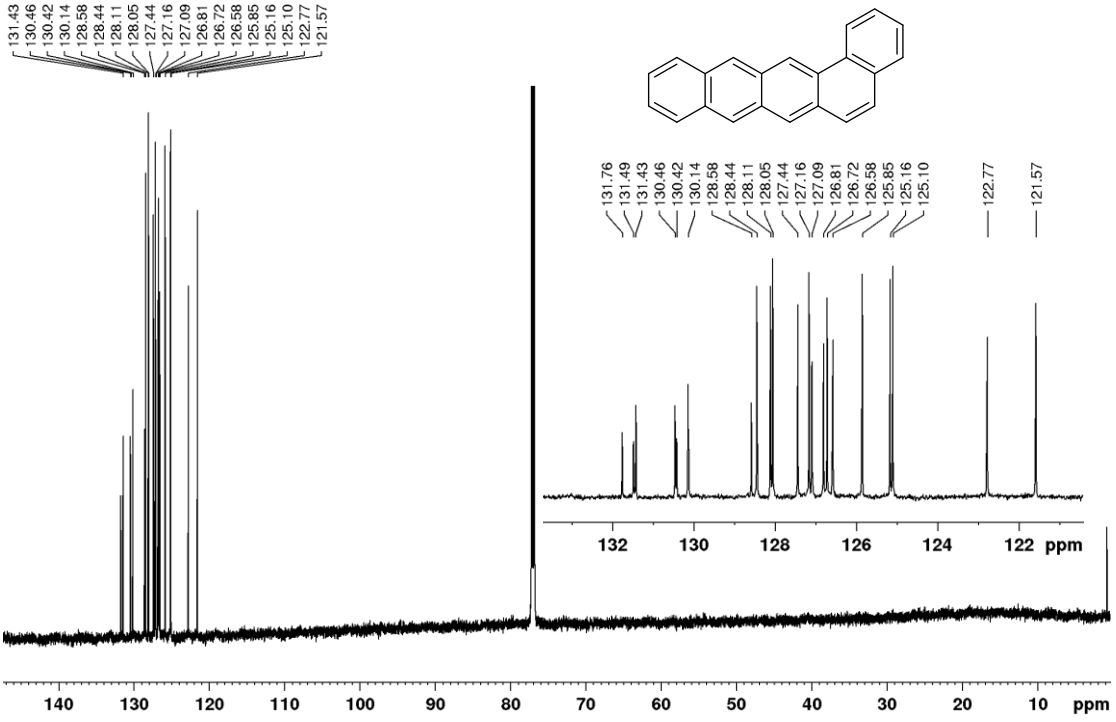

Figure S10: ^{13}C NMR spectrum of benzo[*a*]tetracene (compound **P2**) in $CDCl_3/CS_2$.

Electronic Absorption Spectra

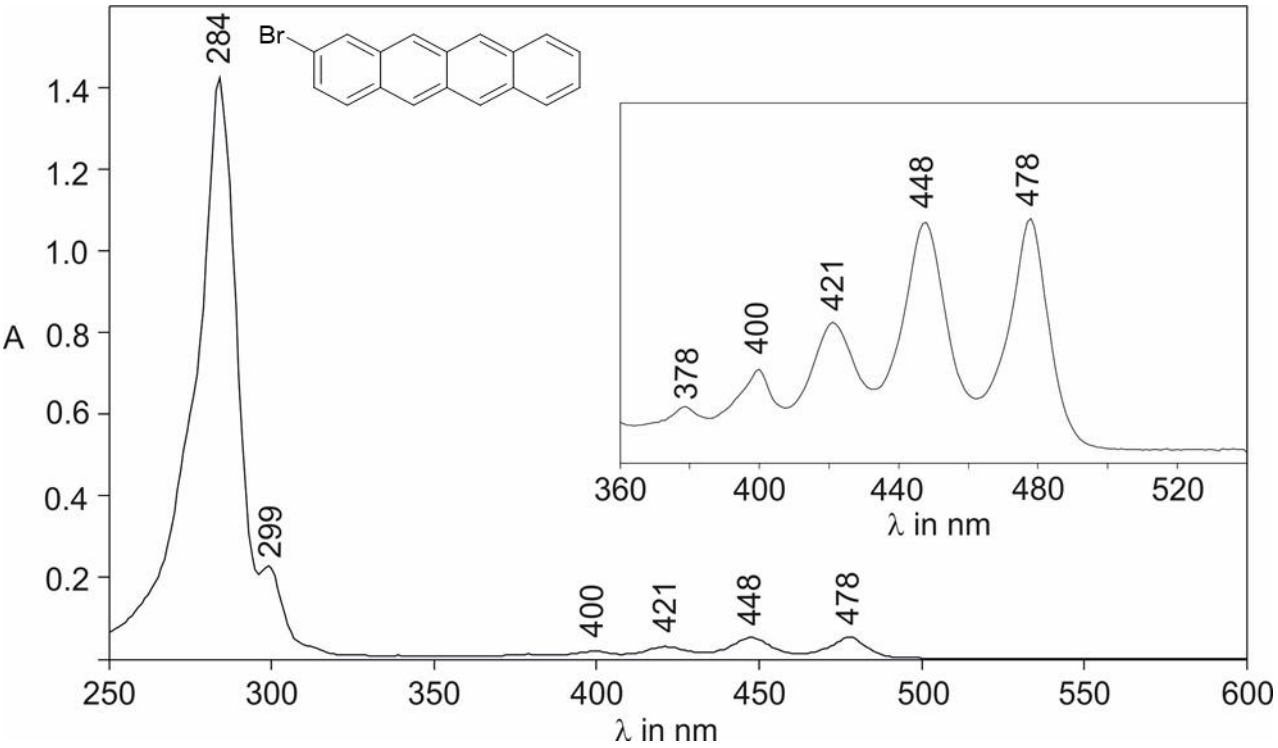

Figure S11: Absorption spectrum of 2-bromotetracene (compound **4**) in $CHCl_3$.

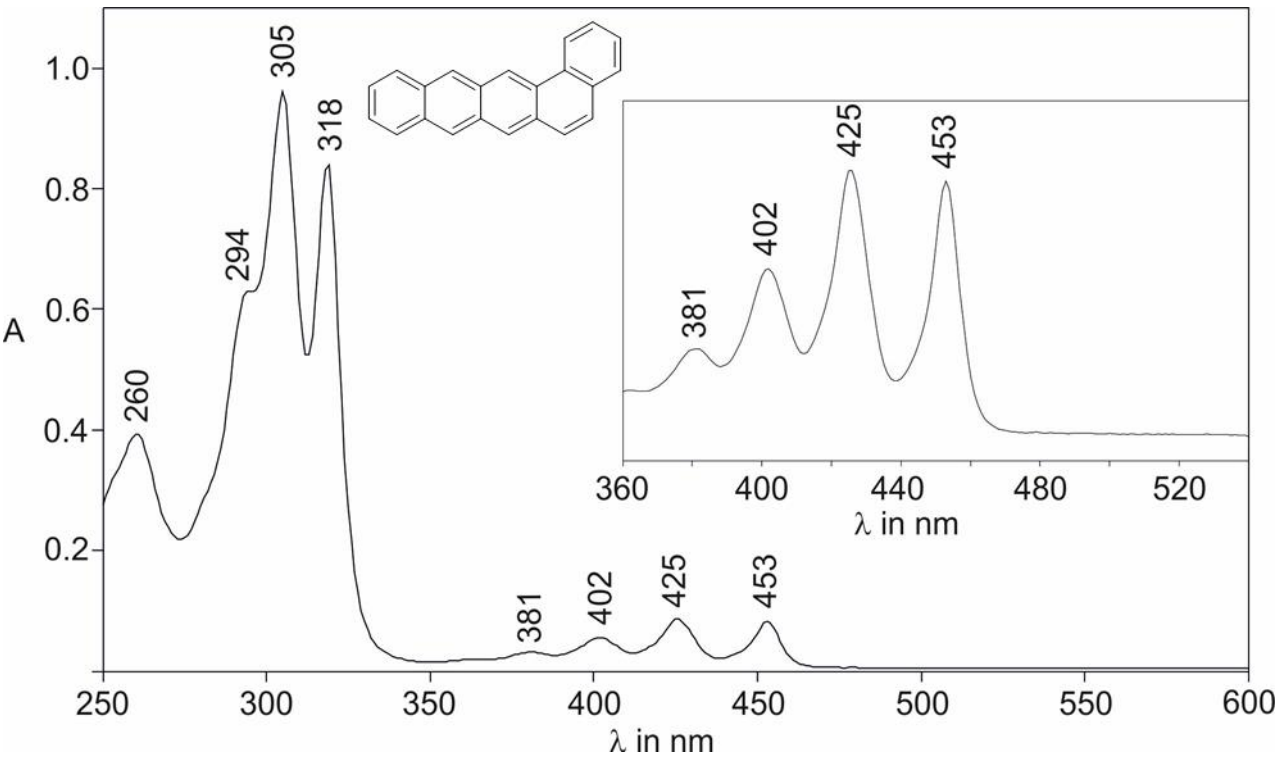

Figure S12: Absorption spectrum of benzo[*a*]tetracene (compound **P2**) in $CHCl_3$ ($c=1.65 \times 10^{-5}$ mol/l).

Table S1. Total energies and zero-point vibrational energies (ZPE) of various species (in hartree) calculated at different levels of theory.

Name	Tetracenyl	C_4H_4	P1	P2	P3	P4	H
ZPE	0.226310	0.060905	0.285615	0.286268	0.281248	0.281863	0
E(B3LYP/6-311G**)	-692.633659	-154.780795	-846.989450	-847.004873	-846.909916	-846.916060	-0.502156
E(RMP2/6-311G**)	-690.531889	-154.288514	-844.425373	-844.443266	-844.340099	-844.344244	-0.499810
E(RMP2/G3Large)	-690.966739	-154.383997	-844.960768	-844.978495	-844.872958	-844.877076	-0.499810
E(CCSD(T)/6-311G**)	-690.723158	-154.344981	-844.654114	-844.671098	-844.574202	-844.577890	-0.499810
E(G3(CC,RMP2)//B3LYP/6-311G**)	-690.931698	-154.379560	-844.903894	-844.920059	-844.825812	-844.828860	-0.499810
Name	**i0a**	**i0b**	**i1**	**i2**	**i3**	**i4**	**i5**
ZPE	0.287577	0.287547	0.290775	0.290879	0.291880	0.295533	0.294573
E(B3LYP/6-311G**)	-847.415638	-847.415812	-847.485884	-847.497554	-847.445487	-847.507822	-847.560976
E(RMP2/6-311G**)	-844.824113	-844.823453	-844.903344	-844.904247	-844.867298	-844.932125	-844.979011
E(RMP2/G3Large)	-845.354853	-845.353986	-845.435478	-845.438041	-845.397936	-845.463615	-845.514553
E(CCSD(T)/6-311G**)	-845.071523	-845.070758	-845.144041	-845.148939	-845.110295	-845.174549	-845.217392
E(G3(CC,RMP2)//B3LYP/6-311G**)	-845.314687	-845.313743	-845.385401	-845.391854	-845.349053	-845.410506	-845.458361
Name	**i6**	**i7**	**i8**	ts i0a-i1	ts i0b-i2	ts i1-i3	tsi1-i6
ZPE	0.291951	0.295447	0.294554	0.287726	0.287310	0.286465	0.286760
E(B3LYP/6-311G**)	-847.445133	-847.502175	-847.558748	-847.413938	-847.411849	-847.421547	-847.422396
E(RMP2/6-311G**)	-844.865385	-844.929034	-844.979822	-844.822773	-844.8201	-844.84079	-844.842665
E(RMP2/G3Large)	-845.396518	-845.460381	-845.515234	-845.354283	-845.351437	-845.373084	-845.374859
E(CCSD(T)/6-311G**)	-845.109008	-845.170707	-845.217358	-845.069329	-845.066108	-845.080196	-845.081738
E(G3(CC,RMP2)//B3LYP/6-311G**)	-845.348190	-845.406607	-845.458215	-845.313112	-845.310136	-845.326025	-845.327171
Name	ts i1-P3	ts i2-P4	ts i3-i4	ts i6-i7	ts i4-i5	ts i7-i8	ts i5-P1
ZPE	0.282407	0.282923	0.291417	0.291429	0.289589	0.289536	0.286608
E(B3LYP/6-311G**)	-847.410163	-847.414689	-847.431462	-847.429282	-847.441203	-847.438393	-847.490212
E(RMP2/6-311G**)	-844.83341	-844.835759	-844.855602	-844.854703	-844.856282	-844.8552	-844.918895
E(RMP2/G3Large)	-845.367549	-845.369639	-845.387062	-845.386075	-845.389905	-845.388678	-845.455428

E(CCSD(T)/6-311G**)	-845.06873	-845.070484	-845.0969	-845.095429	-845.098355	-845.09692	-845.148526
E(G3(CC,RMP2)//B3LYP/6-311G**)	-845.320462	-845.321441	-845.336944	-845.335371	-845.342389	-845.340862	-845.398451
Name	ts i8-P2						
ZPE	0.287690						
E(B3LYP/6-311G**)	-847.503982						
E(RMP2/6-311G**)	-844.933515						
E(RMP2/G3Large)	-845.469897						
E(CCSD(T)/6-311G**)	-845.163149						
E(G3(CC,RMP2)//B3LYP/6-311G**)	-845.411841						

Optimized Cartesian Coordinates (Å) and Vibrational Frequencies (cm^{-1}) of the Reactants, Intermediates, Transition States, and Products Involved in the Reaction Considered

Reactants

Vinylacetylene C_4H_4, C_s, $^1A'$

6	0	0.121125	-1.700404	0.000000
6	0	-0.579921	-0.557132	0.000000
6	0	0.000000	0.743992	0.000000
6	0	0.453986	1.866353	0.000000
1	0	1.206897	-1.705189	0.000000
1	0	-0.382460	-2.662132	0.000000
1	0	-1.669070	-0.596050	0.000000
1	0	0.873491	2.846518	0.000000

Frequencies

229.5891	339.4361	558.9958
588.1117	631.2114	714.7025
899.2819	944.5974	1013.3805
1122.3708	1335.8813	1463.2716
1690.9964	2223.9797	3158.4122
3178.0551	3263.9634	3495.5663

Tetracenyl $C_{18}H_{11}$, C_s, $^2A'$

6	0	4.766321	-1.069443	0.000000
6	0	3.545886	-1.677640	0.000000
6	0	2.337306	-0.908218	0.000000
6	0	2.440046	0.537733	0.000000
6	0	3.744749	1.129746	0.000000
6	0	4.867517	0.356083	0.000000
6	0	1.079472	-1.501028	0.000000
6	0	1.278018	1.300897	0.000000
6	0	0.000000	0.709356	0.000000
6	0	-0.102949	-0.736509	0.000000
6	0	-1.382211	-1.327904	0.000000
6	0	-2.541694	-0.563585	0.000000
6	0	-2.441686	0.885282	0.000000
6	0	-1.182359	1.474763	0.000000
6	0	-3.642312	1.670959	0.000000
6	0	-3.857944	-1.157414	0.000000
6	0	-4.878121	1.080868	0.000000
6	0	-4.915061	-0.327212	0.000000
1	0	-1.459549	-2.410632	0.000000
1	0	1.003587	-2.584050	0.000000
1	0	5.672096	-1.665238	0.000000
1	0	3.469031	-2.759896	0.000000
1	0	3.820647	2.212093	0.000000
1	0	5.848233	0.818172	0.000000
1	0	1.354388	2.383939	0.000000
1	0	-1.104359	2.557603	0.000000
1	0	-3.553217	2.752898	0.000000

1	0	-3.954904	-2.238335	0.000000
1	0	-5.785827	1.673044	0.000000

Frequencies

55.8035	89.7943	151.1166
164.4932	192.7749	270.8226
306.6091	318.0346	320.4994
375.0142	449.3911	454.6502
474.0641	479.6009	503.5193
516.5754	557.5206	559.2622
614.4532	627.8280	643.6932
708.2034	748.5802	750.3509
753.2165	761.8123	773.9106
778.6988	786.2562	825.1169
848.0177	867.1980	867.3511
886.6552	891.6629	913.2364
915.5558	935.4292	965.3929
972.1860	995.9685	1021.6618
1030.7813	1136.1768	1150.5542
1153.1817	1187.3486	1192.6477
1214.1061	1220.4771	1275.9033
1286.6144	1302.0681	1311.5595
1318.6289	1363.9516	1380.7402
1409.2621	1418.8069	1426.7386
1447.4033	1469.5294	1492.5804
1551.0934	1564.0333	1580.6298
1601.7965	1632.7276	1646.9627
1671.7268	3154.0172	3155.2571
3156.3674	3157.5588	3158.0932
3159.5852	3161.3034	3163.4897
3175.6816	3180.4837	3187.6650

Intermediates

Van-der-Waals complex [i0a] $C_{22}H_{15}$, C_1, ^2A

6	0	-6.554770	-0.543686	0.142116
6	0	-5.419488	-1.278200	-0.034026
6	0	-4.128485	-0.657090	-0.020868
6	0	-4.054435	0.775928	0.184721
6	0	-5.275147	1.503954	0.365097
6	0	-6.481683	0.869075	0.344808
6	0	-2.954262	-1.380632	-0.197774
6	0	-2.810282	1.396111	0.200576
6	0	-1.615920	0.671595	0.022310
6	0	-1.689802	-0.761367	-0.183279
6	0	-0.494124	-1.485876	-0.361488
6	0	0.747440	-0.863990	-0.345114
6	0	0.824898	0.571628	-0.139553
6	0	-0.351348	1.291768	0.036972
6	0	2.110110	1.209751	-0.123708
6	0	1.979609	-1.595001	-0.526494
6	0	3.264192	0.493284	-0.298520

6	0	3.126624	-0.895164	-0.492499
6	0	6.802049	-1.310563	1.150712
6	0	7.592487	-0.253697	0.936221
6	0	7.378796	0.721081	-0.078325
6	0	7.233117	1.566137	-0.924970
1	0	-7.524649	-1.028035	0.129594
1	0	-5.474943	-2.350789	-0.187937
1	0	-5.218745	2.576518	0.518972
1	0	-7.397165	1.433179	0.482749
1	0	-3.010758	-2.453869	-0.351728
1	0	-2.754277	2.469409	0.354582
1	0	-0.549070	-2.559005	-0.515459
1	0	-0.297052	2.365040	0.191122
1	0	2.153081	2.283352	0.031692
1	0	1.944478	-2.668321	-0.683140
1	0	4.237337	0.970436	-0.287126
1	0	7.023697	-2.014338	1.943844
1	0	5.920125	-1.496360	0.548727
1	0	8.467554	-0.099341	1.562825
1	0	7.102933	2.301854	-1.680187

Frequencies

5.5362	10.0720	11.9095
24.5583	32.9361	45.6074
58.3303	90.6818	152.2017
164.9399	193.2997	227.8122
271.3644	306.7770	318.2110
319.4199	321.0726	374.7652
449.4157	454.1988	474.0833
479.6200	503.4291	517.0049
557.5733	559.1545	559.7155
614.2581	627.9628	643.6516
645.4735	680.9374	703.5523
707.7373	749.4592	750.4977
753.1917	761.7992	774.5899
783.2327	786.1413	823.7680
847.9778	867.1168	867.3410
886.3519	891.0661	892.2393
913.2641	915.4744	935.2875
964.5949	971.2339	972.2961
995.7981	1009.4834	1021.6524
1030.7356	1112.2977	1137.8895
1150.4502	1155.3327	1187.3258
1192.8922	1213.9825	1220.3887
1276.6469	1286.4974	1301.9798
1311.3952	1318.9559	1322.0557
1364.0150	1380.5773	1409.2662
1418.6865	1426.7876	1445.8554
1447.8383	1469.9007	1492.5901
1550.9353	1563.7903	1580.5985
1601.8466	1632.4898	1646.9653

1668.1338	1671.6756	2202.1073
3135.2283	3143.8092	3153.9545
3155.2286	3156.2095	3157.4667
3157.9821	3159.5317	3161.1351
3163.3580	3175.5345	3180.9836
3187.5490	3233.3874	3476.1939

Van-der-Waals complex [i0b] $C_{22}H_{15}$, C_1, ^2A

6	0	-6.799973	-0.725782	0.133240
6	0	-5.622252	-1.412715	0.112553
6	0	-4.366741	-0.724344	0.063116
6	0	-4.375124	0.724954	0.035386
6	0	-5.637966	1.401271	0.058701
6	0	-6.808162	0.703036	0.105909
6	0	-3.150687	-1.398376	0.041134
6	0	-3.166437	1.410143	-0.012614
6	0	-1.930175	0.736075	-0.035116
6	0	-1.921653	-0.713133	-0.007403
6	0	-0.684137	-1.387234	-0.029878
6	0	0.521689	-0.700283	-0.077635
6	0	0.516741	0.751675	-0.105486
6	0	-0.701110	1.422280	-0.083572
6	0	1.765244	1.457025	-0.154682
6	0	2.960579	0.788935	-0.175831
6	0	2.902044	-0.617930	-0.146996
6	0	1.796033	-1.379622	-0.100997
6	0	6.619068	-0.775876	-0.173625
6	0	7.751145	-0.363112	-0.187184
6	0	9.086827	0.122206	-0.249528
6	0	9.837979	0.415219	0.817156
1	0	-0.677392	-2.472464	-0.009124
1	0	-3.145454	-2.483821	0.061925
1	0	-7.742226	-1.260690	0.170706
1	0	-5.616016	-2.497462	0.133289
1	0	-5.643260	2.486044	0.037915
1	0	-7.756335	1.228372	0.123094
1	0	-3.172140	2.495632	-0.033395
1	0	-0.708508	2.507654	-0.104266
1	0	1.747032	2.542209	-0.175002
1	0	3.905521	1.318092	-0.212664
1	0	1.822729	-2.464247	-0.081139
1	0	5.617988	-1.136583	-0.149481
1	0	9.498104	0.253039	-1.247619
1	0	9.461734	0.296456	1.826267
1	0	10.850630	0.781298	0.699611

Frequencies

2.8844	3.0389	10.2265
18.1095	28.5245	48.9617
56.1781	89.9981	151.4397
165.2000	192.9607	226.0404

271.0158	306.8382	318.4107
320.7680	321.2072	374.2448
449.5644	452.4357	474.1042
479.5787	503.6155	516.4859
557.2488	557.5855	558.7429
614.6683	627.7413	643.5942
687.4574	698.8636	704.4438
706.1866	748.2595	750.1462
753.1504	761.7709	774.1238
779.3950	786.3494	822.9185
848.1396	867.2908	867.4101
886.5538	891.2031	892.8214
913.5042	915.7033	935.3775
953.5269	966.9538	972.5160
996.3576	1010.4347	1021.7036
1030.8055	1111.6723	1136.6893
1150.5789	1154.0571	1187.4754
1192.6249	1214.0761	1220.5372
1275.8007	1286.6270	1302.1371
1311.4560	1318.7834	1321.0314
1363.8146	1380.5698	1409.2016
1418.8257	1426.7388	1443.3444
1447.1523	1469.7288	1492.5642
1550.7259	1563.5485	1580.6488
1602.3246	1632.5237	1646.9197
1668.1124	1671.7406	2200.9260
3134.3362	3146.3916	3154.7350
3156.2377	3157.0719	3158.2510
3159.2730	3160.3773	3162.0188
3163.8800	3175.9263	3183.3783
3187.9006	3235.2765	3445.9209

[i1] $C_{22}H_{15}$, C_1, ^2A

6	0	-6.263752	-0.910152	0.220358
6	0	-5.053291	-1.531571	0.129460
6	0	-3.837928	-0.775824	0.065152
6	0	-3.922098	0.670706	0.098909
6	0	-5.216559	1.276903	0.194719
6	0	-6.346692	0.515994	0.253479
6	0	-2.589810	-1.382048	-0.027858
6	0	-2.752834	1.420946	0.037334
6	0	-1.485176	0.816044	-0.057188
6	0	-1.400626	-0.630898	-0.090809
6	0	-0.131286	-1.235918	-0.185791
6	0	1.036551	-0.485522	-0.248192
6	0	0.950870	0.960077	-0.214956
6	0	-0.294610	1.567473	-0.121163
6	0	2.169961	1.710524	-0.282364
6	0	2.331574	-1.091449	-0.347741
6	0	3.376805	1.087429	-0.373867
6	0	3.473778	-0.345343	-0.412888

6	0	4.844701	-0.987994	-0.518916
6	0	5.698234	-0.730139	0.695906
6	0	6.935818	-0.141431	0.645488
6	0	8.037418	0.384300	0.588697
1	0	-0.068576	-2.319592	-0.210806
1	0	-2.527252	-2.465726	-0.052640
1	0	-7.174939	-1.495710	0.268457
1	0	-4.989887	-2.614460	0.104464
1	0	-5.279036	2.359863	0.219382
1	0	-7.319441	0.989214	0.325972
1	0	-2.816075	2.504584	0.062049
1	0	-0.356715	2.651170	-0.097076
1	0	2.112125	2.793834	-0.259335
1	0	2.387973	-2.175642	-0.376243
1	0	4.289275	1.672218	-0.418787
1	0	4.717435	-2.069932	-0.651305
1	0	5.362837	-0.618693	-1.408947
1	0	5.299593	-1.022605	1.662811
1	0	8.996400	0.838827	0.545381

Frequencies

20.5452	23.7507	49.1599
76.1183	109.5281	128.4645
160.3042	180.0807	193.1186
245.8337	258.3268	290.6013
316.7418	353.8783	369.2798
389.1321	399.7064	448.2239
462.4660	473.8720	477.3235
481.4125	486.7099	520.2828
543.2822	561.1750	597.6259
607.5463	638.5141	646.1441
649.1577	655.3639	733.4839
748.9193	751.7852	763.9314
766.8735	771.3010	778.0851
811.8252	823.4773	846.8904
858.7991	868.7161	881.0445
887.5915	899.0858	916.1278
923.3655	926.9170	972.4123
973.8952	983.7547	995.7310
1021.8328	1026.8966	1141.0882
1147.1979	1150.0770	1166.2610
1172.9557	1187.5982	1202.2261
1204.8954	1223.5375	1229.7218
1290.8429	1295.7337	1298.2664
1317.0400	1319.5797	1345.2706
1368.7969	1397.2022	1401.5144
1412.1043	1425.5749	1438.5510
1465.5990	1473.5025	1487.2812
1501.9996	1556.1806	1578.2490
1582.9734	1611.1275	1648.2415
1664.9385	1678.5405	2013.8815

3003.7631	3061.3222	3151.7972
3151.9745	3154.5790	3156.1617
3157.2162	3158.7996	3159.4087
3160.9518	3163.7267	3175.9843
3178.4163	3187.9593	3468.3210

[i2] $C_{22}H_{15}$, C_1, ^2A

6	0	-5.864807	-1.663035	0.029470
6	0	-4.551111	-2.025083	0.076430
6	0	-3.511316	-1.039793	0.039132
6	0	-3.887589	0.357534	-0.050276
6	0	-5.280926	0.687404	-0.096951
6	0	-6.235554	-0.285540	-0.058562
6	0	-2.164255	-1.379401	0.085871
6	0	-2.892528	1.327985	-0.087717
6	0	-1.525607	0.994201	-0.040946
6	0	-1.148512	-0.403651	0.048992
6	0	0.217795	-0.738233	0.096721
6	0	1.214978	0.233076	0.060318
6	0	0.835599	1.629493	-0.030752
6	0	-0.510104	1.970115	-0.078382
6	0	1.879521	2.608798	-0.068464
6	0	3.189559	2.242486	-0.019166
6	0	3.578793	0.862032	0.073766
6	0	2.601037	-0.100704	0.109836
6	0	5.021184	0.545110	0.127563
6	0	5.565885	-0.639004	0.236993
6	0	6.147623	-1.848691	0.363740
6	0	6.531745	-2.683277	-0.684352
1	0	0.499647	-1.784432	0.164331
1	0	-1.882950	-2.425898	0.152996
1	0	-6.640331	-2.420093	0.058673
1	0	-4.269226	-3.070708	0.143309
1	0	-5.561876	1.733294	-0.163860
1	0	-7.286156	-0.020336	-0.094704
1	0	-3.174500	2.374344	-0.154890
1	0	-0.790928	3.016714	-0.146345
1	0	1.605425	3.656306	-0.137701
1	0	3.966250	2.999604	-0.048679
1	0	2.878363	-1.147774	0.176728
1	0	5.686846	1.409988	0.068746
1	0	6.329499	-2.196892	1.381320
1	0	6.378764	-2.393928	-1.716057
1	0	6.992709	-3.641135	-0.483455

Frequencies

22.1269	38.1072	48.9451
85.0672	111.5307	124.2532
158.9621	174.4802	208.6516
223.7139	264.7284	287.1400
307.5765	332.4447	362.5040

396.5562	408.8140	457.3416
469.1835	474.8214	481.1055
508.3275	530.2579	540.0867
553.7592	581.4630	606.0663
613.8205	639.0326	649.4335
731.0742	744.4775	749.4376
750.1634	762.0274	762.5478
767.8842	774.7784	791.4787
836.3369	839.6969	845.6799
856.2989	877.9800	881.4302
901.7915	913.3078	921.5327
926.8618	934.9498	938.0697
971.5073	976.5409	982.9544
995.1817	1021.4273	1082.4634
1147.6937	1149.8675	1168.1192
1174.4796	1187.5873	1191.2398
1204.9563	1223.4909	1230.9144
1283.1382	1292.1355	1301.1403
1316.5078	1325.7281	1351.0734
1368.4115	1394.2423	1412.1561
1415.9057	1425.3971	1435.5679
1468.3306	1485.6537	1490.5524
1502.6698	1554.3499	1573.8923
1581.3097	1609.0268	1645.6416
1658.3147	1674.2029	1883.8726
3057.6118	3094.0946	3150.0048
3153.5307	3155.1947	3155.9601
3156.9544	3158.4297	3159.2988
3162.5307	3163.6988	3174.5123
3175.2259	3187.2843	3251.0126

[i3] $C_{22}H_{15}$, C_1, ^2A

6	0	-6.204783	-1.237971	0.156823
6	0	-4.949403	-1.754828	0.028588
6	0	-3.798183	-0.902392	0.011966
6	0	-3.995998	0.528058	0.134811
6	0	-5.333801	1.022776	0.267197
6	0	-6.399829	0.172338	0.277990
6	0	-2.506438	-1.400816	-0.117375
6	0	-2.889988	1.371344	0.120632
6	0	-1.579112	0.875700	-0.009792
6	0	-1.381155	-0.554803	-0.132611
6	0	-0.068916	-1.051606	-0.263391
6	0	1.038494	-0.211635	-0.277372
6	0	0.835634	1.219993	-0.154214
6	0	-0.451451	1.722144	-0.025280
6	0	2.002871	2.070389	-0.172336
6	0	2.372560	-0.723709	-0.410177
6	0	3.200336	1.478608	-0.301611
6	0	3.473974	0.094638	-0.428021
6	0	4.884372	-0.423278	-0.561082

6	0	7.101842	-0.642593	0.583630
6	0	8.225525	-1.048913	0.455782
6	0	5.729740	-0.161938	0.710386
1	0	0.077100	-2.123424	-0.355571
1	0	-2.358085	-2.472409	-0.209463
1	0	-7.066676	-1.895509	0.167779
1	0	-4.800524	-2.825613	-0.063495
1	0	-5.481728	2.093690	0.359158
1	0	-7.406605	0.561692	0.378912
1	0	-3.038909	2.442832	0.212647
1	0	-0.598199	2.793779	0.066173
1	0	1.882325	3.145543	-0.084576
1	0	2.502101	-1.798636	-0.504150
1	0	4.866857	-1.495607	-0.768640
1	0	5.376935	0.060835	-1.410017
1	0	9.221299	-1.403570	0.351465
1	0	5.250346	-0.645052	1.568665
1	0	5.736016	0.912419	0.923847

Frequencies

23.9573	38.7664	60.0367
65.8236	95.8368	139.2870
143.8204	167.7279	190.7308
241.6654	249.5154	293.7118
319.3610	339.1133	365.0080
371.3331	385.6851	449.9112
459.8250	470.2127	474.3826
479.6810	513.7921	542.0330
558.8527	600.5031	634.5895
637.3745	646.9351	665.6438
676.8587	708.6682	749.2987
750.4296	753.2696	762.4032
769.4492	772.4966	775.0205
820.9385	829.4174	845.0152
856.0148	872.4045	879.8973
892.2437	913.5906	919.9580
921.4015	941.0629	967.3449
972.0680	996.0264	1015.3628
1021.9566	1029.4413	1144.9266
1149.6667	1173.8721	1186.0003
1189.5954	1198.2185	1214.0697
1226.6612	1258.6375	1284.2534
1289.6244	1302.2083	1306.3468
1314.2455	1319.9283	1360.4195
1368.5509	1388.4292	1402.9337
1421.4200	1424.4316	1439.0078
1470.0948	1476.8776	1491.6714
1494.8282	1553.0904	1567.8360
1581.3362	1607.5536	1638.2352
1647.6437	1671.7023	2221.3785
3022.5961	3039.4774	3052.2399

3089.2419	3144.3584	3154.4880
3155.7351	3156.6209	3157.7086
3159.2593	3161.0400	3163.4439
3175.6985	3187.6900	3477.8852

[i4] $C_{22}H_{15}$, C_1, ^2A

6	0	6.132517	-0.761559	0.074455
6	0	4.948571	-1.438982	0.057482
6	0	3.698687	-0.740827	0.028222
6	0	3.717120	0.707799	0.016980
6	0	4.984800	1.374025	0.035605
6	0	6.150820	0.666702	0.063356
6	0	2.475762	-1.404893	0.010391
6	0	2.512020	1.402686	-0.011310
6	0	1.271129	0.739131	-0.029612
6	0	1.253088	-0.710290	-0.018139
6	0	0.008095	-1.374290	-0.036078
6	0	-1.192253	-0.679748	-0.065097
6	0	-1.175041	0.768822	-0.076713
6	0	0.044588	1.434008	-0.058289
6	0	-2.426494	1.460445	-0.091129
6	0	-2.463143	-1.344676	-0.096209
6	0	-3.620665	0.791498	-0.104168
6	0	-3.639472	-0.659711	-0.128423
6	0	-4.973476	-1.360183	-0.282009
6	0	-6.003819	0.802331	0.241243
6	0	-4.914421	1.497020	-0.038286
6	0	-6.128666	-0.652003	0.475310
1	0	-0.005559	-2.460006	-0.028862
1	0	2.462284	-2.490594	0.018883
1	0	7.070882	-1.304173	0.096554
1	0	4.934094	-2.523922	0.065894
1	0	4.998209	2.458963	0.027162
1	0	7.102822	1.185319	0.077221
1	0	2.526322	2.488342	-0.019721
1	0	0.057855	2.519631	-0.064323
1	0	-2.417372	2.545995	-0.070423
1	0	-2.469303	-2.430813	-0.112760
1	0	-5.233902	-1.366414	-1.348006
1	0	-4.897955	-2.403763	0.034852
1	0	-4.922324	2.576247	-0.163781
1	0	-6.073867	-0.856537	1.552498
1	0	-7.090678	-1.042104	0.129324

Frequencies

36.6663	67.0975	96.0610
119.1292	138.8985	162.3767
227.7477	235.8674	246.3727
262.6874	321.5431	346.7917
363.9834	382.8320	402.6574
453.1723	470.4961	472.5478

477.2661	482.2314	501.0869
542.4775	548.4496	569.7368
627.8494	646.1462	656.8057
700.9068	723.2065	735.0959
750.2702	756.2987	764.8675
766.4589	775.2450	784.6377
821.1178	832.5046	845.2482
849.7965	873.0987	879.4963
892.9321	900.0633	902.0095
916.7436	923.0409	925.6265
936.0907	970.6506	976.9170
994.5382	1020.3525	1022.5888
1134.0067	1151.5083	1154.6260
1176.7849	1187.5889	1198.9595
1199.4072	1208.2397	1224.5105
1231.4561	1253.7081	1290.5168
1294.7517	1312.9475	1316.7427
1320.7157	1323.6198	1350.4598
1367.3697	1393.1969	1407.1173
1424.1101	1442.2595	1466.0205
1474.1034	1475.0442	1477.8347
1493.6263	1554.0087	1578.1725
1582.3811	1610.8924	1645.2546
1663.1380	1674.7118	1681.7240
3001.8625	3009.3872	3053.6232
3068.7004	3141.7755	3148.5687
3152.8850	3154.0447	3155.4118
3156.3728	3157.7031	3159.3495
3162.3294	3174.8094	3186.9759

[i5] $C_{22}H_{15}$, C_s, $^2A"$

6	0	3.783442	-4.905767	0.000000
6	0	3.764881	-3.539813	0.000000
6	0	2.530257	-2.819299	0.000000
6	0	1.292976	-3.569557	0.000000
6	0	1.361561	-4.998544	0.000000
6	0	2.564082	-5.645648	0.000000
6	0	2.480158	-1.424639	0.000000
6	0	0.080916	-2.881511	0.000000
6	0	0.023466	-1.476143	0.000000
6	0	1.264241	-0.725427	0.000000
6	0	1.203811	0.688563	0.000000
6	0	0.000000	1.371175	0.000000
6	0	-1.244155	0.623169	0.000000
6	0	-1.197188	-0.771258	0.000000
6	0	-2.462919	1.345543	0.000000
6	0	-0.072420	2.804467	0.000000
6	0	-2.505536	2.737769	0.000000
6	0	-1.252732	3.481217	0.000000
6	0	-1.278590	5.000795	0.000000
6	0	-3.734137	3.445561	0.000000

6	0	-3.779621	4.857827	0.000000
6	0	-2.645945	5.614125	0.000000
1	0	2.133663	1.249320	0.000000
1	0	3.409383	-0.862846	0.000000
1	0	4.728069	-5.437869	0.000000
1	0	4.692421	-2.976693	0.000000
1	0	0.433468	-5.560721	0.000000
1	0	2.599858	-6.729248	0.000000
1	0	-0.847502	-3.444522	0.000000
1	0	-2.126707	-1.332218	0.000000
1	0	-3.396397	0.791093	0.000000
1	0	0.864172	3.356110	0.000000
1	0	-0.717435	5.374147	0.869302
1	0	-0.717435	5.374147	-0.869302
1	0	-4.658797	2.879390	0.000000
1	0	-4.748073	5.347387	0.000000
1	0	-2.707975	6.696889	0.000000

Frequencies

34.2274	50.6419	81.5176
116.4370	118.4234	156.1042
220.2036	237.2743	241.7430
259.6944	335.0895	347.5361
360.5197	393.0157	450.6435
459.4596	473.3230	476.1088
478.6440	484.9548	507.5671
545.6887	573.1846	582.8532
630.7587	644.7639	649.6093
674.8892	714.5608	725.8376
736.2211	750.2653	754.9875
763.1437	772.8901	786.1390
795.7206	833.8085	837.7658
843.7462	862.2099	880.3835
884.9730	890.0379	906.0713
909.2138	914.4283	929.9101
953.1674	955.5847	968.1865
970.3737	992.8717	1024.8936
1073.2489	1142.1750	1149.1874
1160.6227	1184.9811	1186.4046
1188.9409	1202.4247	1211.2446
1227.2726	1240.1003	1289.9932
1292.8471	1302.4998	1313.2138
1316.3500	1323.5277	1360.3775
1375.9929	1401.8294	1405.3806
1418.6473	1423.3074	1437.6638
1447.7771	1464.1331	1488.6652
1496.2551	1527.7529	1549.2413
1574.7057	1579.3468	1607.4399
1626.2735	1647.4694	1666.3406
2973.5632	2979.8805	3140.9063
3152.3943	3153.4475	3154.2069

3155.1424	3156.2162	3157.3331
3159.4272	3162.0928	3170.0746
3174.5149	3180.7353	3186.8224

[i6] $C_{22}H_{15}$, C_s, $^2A'$

6	0	6.004426	-1.579785	-0.000088
6	0	4.701424	-1.982218	0.000030
6	0	3.633910	-1.027146	0.000024
6	0	3.968610	0.382792	-0.000123
6	0	5.351527	0.755826	-0.000246
6	0	6.334422	-0.189627	-0.000227
6	0	2.296270	-1.408108	0.000170
6	0	2.944772	1.324334	-0.000130
6	0	1.588587	0.948255	0.000012
6	0	1.253664	-0.462443	0.000187
6	0	-0.103634	-0.843249	0.000400
6	0	-1.120612	0.102082	0.000348
6	0	-0.789700	1.522063	0.000134
6	0	0.546025	1.898037	0.000007
6	0	-1.869091	2.468086	0.000121
6	0	-2.501677	-0.195115	0.000414
6	0	-3.170919	2.069782	0.000145
6	0	-3.536099	0.667752	0.000020
6	0	-4.996103	0.277144	-0.000443
6	0	-6.649373	-1.593326	-0.000138
6	0	-7.820467	-1.862846	-0.000045
6	0	-5.232370	-1.243561	-0.000289
1	0	-0.359627	-1.896908	0.000594
1	0	2.045446	-2.464361	0.000281
1	0	6.801870	-2.314231	-0.000077
1	0	4.450193	-3.037688	0.000136
1	0	5.601883	1.811558	-0.000356
1	0	7.376921	0.108011	-0.000314
1	0	3.195853	2.380618	-0.000256
1	0	0.799511	2.953950	-0.000067
1	0	-1.624639	3.524959	0.000147
1	0	-3.967688	2.807892	0.000293
1	0	-5.487986	0.718546	0.873587
1	0	-5.487046	0.718192	-0.875207
1	0	-8.853733	-2.108922	0.000121
1	0	-4.746174	-1.686907	0.875508
1	0	-4.746328	-1.687079	-0.876083

Frequencies

32.6567	38.9755	54.6266
58.6168	90.6034	127.6826
146.2034	170.6133	173.6594
227.8812	278.2670	285.5055
312.8205	337.4489	353.9201
376.1888	389.5499	438.7435
471.4678	477.1628	482.1409

501.4283	516.1991	530.6741
559.9671	568.5251	605.0875
638.4261	645.8457	662.9695
676.2594	717.7501	748.3471
748.5944	752.1552	763.3941
767.2625	769.4674	774.7033
803.3639	836.9624	848.5075
863.6169	877.0377	884.8444
912.4785	916.1111	927.8898
952.5486	965.8953	972.7117
989.0566	996.8883	1022.2758
1034.2534	1035.5454	1139.3397
1149.9076	1152.8887	1174.2605
1188.7073	1197.8479	1205.4941
1221.5420	1242.6865	1271.8103
1297.1603	1302.7198	1310.4703
1311.9541	1320.8642	1360.2330
1380.3123	1388.8975	1406.7578
1411.3934	1430.0290	1448.2555
1473.4781	1483.0933	1487.3662
1491.4750	1543.1038	1559.7088
1581.3333	1611.2737	1645.7034
1665.2854	1676.7350	2222.3905
3019.0394	3028.7049	3040.3237
3063.0488	3150.1373	3154.2060
3156.9321	3158.9373	3159.3095
3163.8666	3174.0917	3174.5700
3176.4828	3188.5646	3477.2663

[i7] $C_{22}H_{15}$, C_1, ^2A

6	0	5.751104	-1.281844	0.017719
6	0	4.471047	-1.750426	-0.016111
6	0	3.354877	-0.852122	-0.009689
6	0	3.616410	0.573368	0.033794
6	0	4.978624	1.016403	0.068212
6	0	6.008885	0.123300	0.060507
6	0	2.039542	-1.301502	-0.043884
6	0	2.545883	1.460129	0.041344
6	0	1.211044	1.012342	0.006944
6	0	0.948818	-0.410701	-0.038432
6	0	-0.386296	-0.860612	-0.074464
6	0	-1.468082	0.014573	-0.073549
6	0	-1.198779	1.440919	-0.015347
6	0	0.115402	1.894107	0.020328
6	0	-2.301061	2.349513	0.011734
6	0	-2.845419	-0.428237	-0.119716
6	0	-3.583988	1.889524	-0.014366
6	0	-3.873466	0.495521	-0.078935
6	0	-5.314424	0.033819	-0.191363
6	0	-4.438559	-2.226050	0.079858
6	0	-3.199288	-1.866145	-0.202652

6	0	-5.561131	-1.343721	0.468556
1	0	-0.551927	-1.930441	-0.094577
1	0	1.844875	-2.369203	-0.076736
1	0	6.585430	-1.974159	0.012379
1	0	4.275001	-2.817106	-0.048611
1	0	5.173784	2.083254	0.100695
1	0	7.034514	0.473771	0.086855
1	0	2.740555	2.527759	0.075124
1	0	0.301997	2.962822	0.063494
1	0	-2.096310	3.413644	0.058722
1	0	-4.411514	2.591323	0.009577
1	0	-5.988245	0.778797	0.241184
1	0	-5.569446	-0.042253	-1.257536
1	0	-2.442317	-2.593794	-0.470939
1	0	-6.530379	-1.740726	0.153872
1	0	-5.592868	-1.256636	1.563569

Frequencies

42.5180	58.9129	94.9977
120.5468	129.6995	172.4701
186.7579	231.8876	267.3398
292.4021	293.8065	343.3816
363.3985	381.9564	409.5785
437.9047	472.1342	476.8068
480.5847	501.9270	506.1302
539.2855	552.1875	573.5061
597.9519	618.0756	642.1666
687.0117	719.1952	735.6489
749.4268	756.1073	762.5582
766.7667	774.0419	796.8282
808.0421	828.4955	845.7083
846.6486	859.6267	881.2336
883.0622	909.9049	913.3041
914.1357	929.4474	968.4828
971.4684	979.9175	986.9981
995.0727	1018.1159	1021.4210
1098.9375	1148.8940	1151.7983
1168.8859	1187.2619	1191.8836
1196.4633	1208.8087	1223.1296
1233.3666	1249.7180	1273.7312
1304.2505	1308.7178	1317.7340
1324.8504	1347.2988	1364.2396
1371.1911	1392.3015	1412.7605
1419.0032	1429.2171	1455.4815
1464.7341	1474.2961	1483.2090
1499.3438	1550.8681	1560.0463
1580.9909	1607.0662	1644.3333
1647.1909	1671.8242	1683.8069
2987.8176	2997.5767	3058.8436
3062.0096	3153.3996	3154.3534
3155.5265	3157.2001	3158.3687

3162.4002	3167.2813	3174.9338
3175.0853	3187.1188	3189.6028

[i8] $C_{22}H_{15}$, C_s, $^2A"$

6	0	-5.766908	-1.223270	0.000000
6	0	-4.792966	-0.267014	0.000000
6	0	-3.407565	-0.624931	0.000000
6	0	-3.057121	-2.029800	0.000000
6	0	-4.113252	-2.996143	0.000000
6	0	-5.421670	-2.608321	0.000000
6	0	-2.391969	0.329312	0.000000
6	0	-1.713270	-2.395116	0.000000
6	0	-0.685499	-1.435407	0.000000
6	0	-1.034795	-0.032696	0.000000
6	0	0.000000	0.931412	0.000000
6	0	1.341775	0.588200	0.000000
6	0	1.685800	-0.822175	0.000000
6	0	0.680237	-1.780896	0.000000
6	0	3.064703	-1.198258	0.000000
6	0	2.420848	1.582363	0.000000
6	0	4.048866	-0.248994	0.000000
6	0	3.755406	1.136301	0.000000
6	0	4.911971	2.113041	0.000000
6	0	2.159802	2.975075	0.000000
6	0	3.208761	3.927480	0.000000
6	0	4.515462	3.555210	0.000000
1	0	-0.298329	1.972258	0.000000
1	0	-2.655747	1.382647	0.000000
1	0	-6.812460	-0.936514	0.000000
1	0	-5.054745	0.786003	0.000000
1	0	-3.850451	-4.048880	0.000000
1	0	-6.210509	-3.352102	0.000000
1	0	-1.449508	-3.448342	0.000000
1	0	0.955629	-2.831088	0.000000
1	0	3.315460	-2.253383	0.000000
1	0	5.090297	-0.556917	0.000000
1	0	5.561074	1.907628	0.867586
1	0	5.561074	1.907628	-0.867586
1	0	1.141765	3.338030	0.000000
1	0	2.950314	4.981520	0.000000
1	0	5.304443	4.299277	0.000000

Frequencies

43.6578	48.5990	91.3068
109.2206	118.5403	156.3446
184.0125	231.0120	260.3658
289.4348	299.4394	342.6412
377.7183	392.4977	444.1647
465.1705	471.9477	476.5876
477.4816	506.9025	528.1720
533.2555	545.0077	599.2394

614.1039	620.0557	642.9779
670.8861	712.1480	726.2827
733.1693	744.6076	751.1445
765.5665	773.0472	791.8843
795.5440	803.8186	845.9076
847.9368	855.9136	879.0832
884.2049	907.3545	910.3207
929.5032	936.0243	945.6559
963.5614	969.3321	970.1667
989.3709	994.4791	1023.7903
1074.1231	1127.5281	1151.3624
1154.5245	1181.9076	1186.0401
1189.4105	1202.6091	1204.1409
1219.4590	1232.4305	1251.5766
1280.2527	1295.3301	1308.4079
1316.6992	1319.9877	1370.2389
1377.6643	1390.3646	1412.6264
1424.4283	1431.8751	1441.5337
1448.7858	1458.7469	1485.7752
1502.8541	1522.0720	1558.4767
1581.0641	1588.6099	1600.9415
1627.9822	1645.0048	1669.3602
2935.8382	2939.6780	3148.8587
3153.5824	3153.9765	3154.9999
3156.9743	3158.2851	3162.2200
3174.1341	3174.5179	3174.8796
3183.7709	3187.0775	3210.8424

Products

Pentacene P1 $C_{22}H_{14}$, D_{2h}, $^1A_1$

6	0	0.000000	0.715877	-6.108056
6	0	0.000000	1.408418	-4.935298
6	0	0.000000	0.726752	-3.672673
6	0	0.000000	-0.726752	-3.672673
6	0	0.000000	-1.408418	-4.935298
6	0	0.000000	-0.715877	-6.108056
6	0	0.000000	1.406070	-2.464267
6	0	0.000000	-1.406070	-2.464267
6	0	0.000000	-0.727500	-1.224502
6	0	0.000000	0.727500	-1.224502
6	0	0.000000	1.406570	0.000007
6	0	0.000000	0.727498	1.224499
6	0	0.000000	-0.727498	1.224499
6	0	0.000000	-1.406570	0.000007
6	0	0.000000	-1.406075	2.464280
6	0	0.000000	1.406075	2.464280
6	0	0.000000	-0.726749	3.672667
6	0	0.000000	0.726749	3.672667
6	0	0.000000	-1.408430	4.935300
6	0	0.000000	-0.715886	6.108042
6	0	0.000000	0.715886	6.108042

6	0	0.000000	1.408430	4.935300
1	0	0.000000	2.492186	0.000014
1	0	0.000000	2.491786	-2.464840
1	0	0.000000	1.245313	-7.054147
1	0	0.000000	2.493428	-4.935053
1	0	0.000000	-2.493428	-4.935053
1	0	0.000000	-1.245313	-7.054147
1	0	0.000000	-2.491786	-2.464840
1	0	0.000000	-2.492186	0.000014
1	0	0.000000	-2.491790	2.464840
1	0	0.000000	2.491790	2.464840
1	0	0.000000	-2.493438	4.935040
1	0	0.000000	-1.245283	7.054154
1	0	0.000000	1.245283	7.054154
1	0	0.000000	2.493438	4.935040

Frequencies

36.9372	70.8468	101.3342
118.8825	148.6387	192.5705
238.2499	240.3757	263.5255
293.1078	348.8996	362.0635
379.0631	453.9768	469.3631
471.2086	476.5719	478.3173
490.8600	512.5213	526.0945
553.7031	579.0195	616.3955
639.3335	647.1557	715.7635
724.8646	744.2496	745.5198
751.5275	752.3959	761.9549
770.6333	774.2176	795.3146
837.4540	839.8434	840.1706
846.9556	874.0640	887.7721
889.0408	900.6767	915.6712
921.1544	922.0935	936.3605
972.3674	972.8098	995.1909
995.2180	1016.2102	1018.9658
1134.3424	1143.6215	1158.0467
1184.5370	1188.1129	1200.2043
1207.2872	1210.1757	1242.1231
1251.0512	1294.5554	1295.2730
1312.3943	1318.6447	1333.5980
1359.0245	1376.1037	1410.6469
1416.9080	1418.8759	1426.6966
1434.0870	1477.2417	1477.8486
1493.1196	1542.4239	1557.6422
1576.5291	1578.7263	1593.8411
1633.4264	1641.8767	1672.7733
1673.6068	3153.5900	3154.9265
3155.3207	3157.0020	3157.0494
3158.0236	3159.4871	3160.4334
3162.5764	3163.5120	3175.4898
3175.5256	3187.3770	3187.5640

Benzo[a]tetraphene P2 $C_{22}H_{14}$, C_s, $^1A'$

6	0	5.687699	-1.398107	0.000000
6	0	4.748835	-0.407302	0.000000
6	0	3.351634	-0.715518	0.000000
6	0	2.951374	-2.106145	0.000000
6	0	3.971227	-3.109878	0.000000
6	0	5.293030	-2.769463	0.000000
6	0	2.370523	0.274767	0.000000
6	0	1.594076	-2.422793	0.000000
6	0	0.603790	-1.427526	0.000000
6	0	1.002199	-0.039360	0.000000
6	0	0.000000	0.960520	0.000000
6	0	-1.350396	0.662296	0.000000
6	0	-1.743319	-0.733081	0.000000
6	0	-0.777140	-1.723989	0.000000
6	0	-3.144625	-1.069449	0.000000
6	0	-2.398391	1.690008	0.000000
6	0	-4.099086	-0.113353	0.000000
6	0	-3.762001	1.289870	0.000000
6	0	-2.116095	3.069325	0.000000
6	0	-3.126692	4.015387	0.000000
6	0	-4.468617	3.614967	0.000000
6	0	-4.775418	2.267449	0.000000
1	0	0.332625	1.991257	0.000000
1	0	2.671745	1.317978	0.000000
1	0	6.742875	-1.149114	0.000000
1	0	5.048328	0.635585	0.000000
1	0	3.670628	-4.152431	0.000000
1	0	6.054504	-3.541201	0.000000
1	0	1.292703	-3.465874	0.000000
1	0	-1.088502	-2.764080	0.000000
1	0	-3.416294	-2.119801	0.000000
1	0	-5.149498	-0.384976	0.000000
1	0	-1.089097	3.411196	0.000000
1	0	-2.875122	5.069934	0.000000
1	0	-5.259510	4.356279	0.000000
1	0	-5.811023	1.943499	0.000000

Frequencies

44.1736	54.4339	102.7990
120.0102	140.9920	188.5516
224.7742	233.3061	293.6493
299.5456	324.3628	381.8416
393.6462	427.8326	457.5052
471.9078	478.4864	483.1927
518.4402	529.4142	547.2540
549.5905	565.0876	599.8269
639.6480	647.2516	687.9259
724.1310	745.7262	750.8900
753.3808	756.5726	767.9241

774.6218	791.6178	799.7369
815.4288	847.7844	849.6218
861.5627	877.9879	885.5935
891.2456	909.4221	914.6000
930.3841	953.5218	970.8012
981.4381	991.6796	995.3913
1002.0849	1024.8017	1065.8179
1127.9428	1150.7233	1157.7254
1173.5944	1188.0515	1190.1082
1208.1110	1221.6459	1233.9241
1255.3616	1270.5259	1298.3613
1306.4595	1318.2576	1325.9889
1350.0025	1374.1236	1383.0926
1416.1358	1425.3049	1445.6003
1449.3924	1471.9771	1486.8965
1499.4567	1526.4593	1562.5100
1585.3778	1592.2781	1616.0674
1641.8422	1656.8347	1661.3940
1672.7266	3153.8297	3154.7902
3156.1502	3157.5007	3158.6350
3159.5841	3162.6278	3168.6709
3175.2104	3175.6994	3178.8544
3186.0460	3187.3576	3198.7592

(E)-2-(but-1-en-3-yn-1-yl)anthracene P3 $C_{22}H_{14}$, C_1, ^1A

6	0	-6.014631	-1.501344	0.002463
6	0	-4.721109	-1.931437	-0.027723
6	0	-3.632688	-0.999643	-0.015223
6	0	-3.937008	0.417076	0.030458
6	0	-5.311486	0.819090	0.060969
6	0	-6.314442	-0.104779	0.047510
6	0	-2.304587	-1.408873	-0.045299
6	0	-2.893610	1.336547	0.043138
6	0	-1.545932	0.932265	0.012795
6	0	-1.240891	-0.485159	-0.032904
6	0	0.106520	-0.890207	-0.063453
6	0	1.151768	0.030199	-0.048615
6	0	0.844327	1.446296	-0.005414
6	0	-0.481542	1.856234	0.024074
6	0	1.938219	2.370936	-0.001921
6	0	2.517853	-0.376496	-0.078837
6	0	3.226463	1.936159	-0.032279
6	0	3.550951	0.532542	-0.060920
6	0	4.964223	0.157919	-0.079220
6	0	5.481251	-1.070592	0.127572
6	0	6.866550	-1.359750	0.083012
6	0	8.039045	-1.641208	0.054877
1	0	0.334471	-1.951099	-0.097712
1	0	-2.076850	-2.469847	-0.079466
1	0	-6.827869	-2.218192	-0.007535
1	0	-4.492909	-2.991583	-0.061964

1	0	-5.538817	1.879430	0.095191
1	0	-7.350163	0.214700	0.070968
1	0	-3.122090	2.397380	0.077343
1	0	-0.708850	2.917346	0.056380
1	0	1.718749	3.433090	0.023694
1	0	2.724535	-1.439900	-0.132344
1	0	4.040467	2.653232	-0.028583
1	0	5.661599	0.970017	-0.265897
1	0	4.828529	-1.909842	0.352777
1	0	9.073732	-1.879384	0.026782

Frequencies

26.6679	49.2484	60.5563
77.7112	94.4860	141.7307
150.3625	184.6056	191.7577
239.5879	282.7773	296.1399
321.1535	346.7392	384.7901
396.8010	441.8867	453.1841
471.6293	475.8071	481.7743
503.0620	523.2069	541.8448
571.4904	618.1581	624.4885
628.2921	639.0155	649.5312
680.9279	732.0417	750.6111
757.7040	763.5156	765.1915
775.1462	776.9621	807.0585
844.4545	851.0127	854.7858
868.2697	882.9391	885.4167
897.8008	914.0552	921.9064
929.7278	972.3753	976.5251
984.4502	990.8747	996.3091
1021.6645	1037.2900	1149.2249
1150.2928	1169.3410	1183.8589
1188.2008	1205.7256	1224.1685
1236.0678	1284.4326	1294.3901
1301.5922	1318.4373	1324.7743
1330.8759	1355.7999	1370.1036
1400.0149	1412.9240	1425.3388
1436.8770	1465.5169	1486.2760
1500.6508	1553.2780	1573.6081
1581.2488	1609.6577	1636.7816
1649.4940	1668.3141	1679.9734
2193.2758	3138.6778	3150.6863
3154.4346	3156.1511	3157.1124
3158.6464	3159.3586	3160.4300
3163.5802	3168.4957	3175.9712
3177.1754	3187.8504	3477.2352

2-(but-3-en-1-yn-1-yl)anthracene P4 $C_{22}H_{14}$, C_s, $^1A'$

6	0	-6.124511	1.632576	0.000000
6	0	-4.832433	2.068472	0.000000
6	0	-3.740471	1.141059	0.000000

6	0	-4.039081	-0.277305	0.000000
6	0	-5.411876	-0.685592	0.000000
6	0	-6.418735	0.234316	0.000000
6	0	-2.413500	1.556236	0.000000
6	0	-2.991608	-1.192718	0.000000
6	0	-1.645853	-0.782210	0.000000
6	0	-1.346660	0.636821	0.000000
6	0	0.000000	1.047842	0.000000
6	0	1.047379	0.131284	0.000000
6	0	0.746764	-1.286920	0.000000
6	0	-0.577164	-1.702247	0.000000
6	0	1.843287	-2.210985	0.000000
6	0	3.132141	-1.780208	0.000000
6	0	3.442560	-0.370208	0.000000
6	0	2.412711	0.544079	0.000000
6	0	4.799585	0.047782	0.000000
6	0	5.966615	0.374806	0.000000
6	0	7.314978	0.808669	0.000000
6	0	8.381869	-0.002178	0.000000
1	0	0.224650	2.109881	0.000000
1	0	-2.189841	2.618617	0.000000
1	0	-6.940616	2.346232	0.000000
1	0	-4.608388	3.130056	0.000000
1	0	-5.634986	-1.747381	0.000000
1	0	-7.453246	-0.089923	0.000000
1	0	-3.215883	-2.254997	0.000000
1	0	-0.800658	-2.764653	0.000000
1	0	1.623451	-3.273401	0.000000
1	0	3.952686	-2.487077	0.000000
1	0	2.637719	1.604439	0.000000
1	0	7.466821	1.885814	0.000000
1	0	8.275905	-1.080443	0.000000
1	0	9.386395	0.402609	0.000000

Frequencies

26.1855	43.7681	47.9848
68.7893	98.5270	139.2949
147.3350	183.6825	185.1830
238.0450	270.7992	289.2601
303.8224	332.4359	381.7322
396.5283	433.6815	452.6053
470.2034	475.5807	481.7993
505.4047	532.8421	543.4869
572.4181	600.2050	625.7497
639.7826	651.5762	686.6932
693.8760	732.2319	750.8424
760.7626	764.0523	764.9697
775.5398	809.1175	814.3872
845.9089	857.0171	870.0979
881.7916	900.4754	910.6590
914.7152	925.0959	938.4746

939.3666	972.3544	981.6899
988.4120	996.2921	1006.1574
1022.0441	1095.1126	1150.3029
1150.6608	1164.2407	1188.0843
1203.5719	1219.4988	1223.9479
1268.6251	1292.3478	1298.8069
1316.1341	1319.2928	1322.8545
1335.2892	1369.0080	1392.1462
1411.8716	1424.1517	1434.2674
1448.8354	1463.1984	1487.7687
1499.1501	1549.4891	1569.9822
1581.1635	1608.6482	1645.4987
1650.8284	1666.4986	1674.7921
2290.7146	3129.4830	3146.2034
3154.6853	3156.5479	3157.6240
3159.1814	3160.6317	3163.5074
3164.8821	3175.9351	3179.2717
3187.9019	3193.2977	3235.7605

Transition states

[i0a] → [i1] $C_{22}H_{15}$, C_1, ^2A

6	0	-6.404207	-0.777460	-0.078251
6	0	-5.213503	-1.441672	-0.100588
6	0	-3.970266	-0.731143	-0.053775
6	0	-4.005260	0.716219	0.018216
6	0	-5.280844	1.368261	0.039191
6	0	-6.438619	0.649460	-0.007282
6	0	-2.741483	-1.381718	-0.075122
6	0	-2.808776	1.422739	0.064351
6	0	-1.559778	0.772534	0.043153
6	0	-1.524590	-0.674827	-0.028764
6	0	-0.274230	-1.324777	-0.049891
6	0	0.919896	-0.617033	-0.003791
6	0	0.887460	0.832825	0.068038
6	0	-0.342764	1.480267	0.089312
6	0	2.124857	1.557853	0.114997
6	0	2.206698	-1.270638	-0.024699
6	0	3.329936	0.909195	0.094689
6	0	3.308661	-0.498741	0.022914
6	0	5.688583	-1.590366	-0.051512
6	0	6.532417	-0.743847	0.572921
6	0	7.228192	0.309597	-0.071210
6	0	7.832302	1.216603	-0.588767
1	0	-7.336802	-1.329190	-0.114320
1	0	-5.187346	-2.525030	-0.154488
1	0	-5.306031	2.451658	0.093072
1	0	-7.396590	1.156793	0.009331
1	0	-2.716360	-2.465812	-0.129076
1	0	-2.834457	2.506852	0.118233
1	0	-0.247809	-2.408737	-0.103872
1	0	-0.369847	2.564288	0.142979

1	0	2.087261	2.641655	0.167953
1	0	2.246294	-2.354408	-0.079775
1	0	4.266632	1.453666	0.129631
1	0	5.226028	-2.404384	0.490754
1	0	5.547785	-1.559124	-1.124075
1	0	6.688334	-0.836533	1.644537
1	0	8.364831	2.008323	-1.055662

Frequencies

-101.7589	10.9760	21.8358
28.8085	58.5803	67.7566
91.6005	149.0297	165.0594
179.0331	196.1012	228.0040
272.3726	308.7512	314.9935
321.1280	360.0087	376.2103
450.0875	457.6085	474.0724
479.6673	499.6394	517.6322
554.7183	559.2133	560.5522
607.9874	628.1366	631.4683
643.8372	677.6176	714.1928
718.2564	749.4845	752.5026
754.0041	761.6517	774.6341
782.1919	785.0376	827.3795
848.0662	865.5390	867.5427
874.2616	886.5852	895.5697
913.1595	915.2998	923.5560
938.0606	971.1084	972.1091
984.9915	995.4402	1021.6235
1031.6276	1112.8462	1138.5594
1150.2963	1154.8419	1187.3121
1194.2101	1214.8932	1220.4745
1279.7361	1286.9945	1302.3867
1305.7732	1311.4643	1319.2862
1364.2946	1381.6278	1409.3369
1418.8805	1426.9291	1436.2651
1449.3820	1469.3157	1492.8173
1552.2203	1565.4900	1580.6136
1596.8292	1609.0514	1632.3660
1646.8453	1671.5883	2184.0708
3140.6387	3148.5991	3153.1810
3154.2601	3155.8129	3155.9185
3157.0516	3158.6753	3159.9816
3162.9416	3175.3129	3179.6626
3187.3746	3248.7783	3475.7889

[i0b] → [i2] $C_{22}H_{15}$, C_1, ^2A

6	0	-6.195099	-1.284610	0.171794
6	0	-4.948852	-1.763051	-0.106515
6	0	-3.800732	-0.907414	-0.056819
6	0	-3.993094	0.484998	0.297450
6	0	-5.321679	0.940107	0.581116

6	0	-6.384645	0.088153	0.521011
6	0	-2.518460	-1.367526	-0.335435
6	0	-2.890643	1.330355	0.350929
6	0	-1.588430	0.873343	0.070529
6	0	-1.395793	-0.519077	-0.283774
6	0	-0.092352	-0.975629	-0.564226
6	0	1.008198	-0.129782	-0.510260
6	0	0.817486	1.265174	-0.155151
6	0	-0.465769	1.722500	0.122631
6	0	1.959098	2.132516	-0.098409
6	0	3.216672	1.668457	-0.373916
6	0	3.354034	0.307510	-0.721658
6	0	2.347507	-0.584969	-0.793844
6	0	5.673899	-0.491749	-1.260579
6	0	6.334494	-0.522172	-0.241983
6	0	7.039187	-0.492352	0.983759
6	0	7.053285	-1.491091	1.878856
1	0	0.052091	-2.018431	-0.829444
1	0	-2.375383	-2.410628	-0.600603
1	0	-7.054215	-1.944647	0.129974
1	0	-4.804868	-2.805300	-0.371634
1	0	-5.464690	1.982530	0.846159
1	0	-7.384307	0.447111	0.738357
1	0	-3.034253	2.373382	0.616271
1	0	-0.610608	2.765177	0.388483
1	0	1.804657	3.173085	0.170701
1	0	4.079577	2.323105	-0.328104
1	0	2.506626	-1.627249	-1.053659
1	0	5.311256	-0.562581	-2.257146
1	0	7.603482	0.415013	1.186005
1	0	6.503031	-2.409305	1.712713
1	0	7.617746	-1.403423	2.798891

Frequencies

-192.1378	4.4244	14.2102
37.7887	46.1742	64.4743
88.1897	101.1469	155.5617
167.5330	194.7001	229.4990
271.5916	304.4772	308.0949
319.8718	337.1152	376.7403
449.7755	459.9058	473.9231
479.6643	494.2300	517.1892
548.7693	560.8675	561.4251
595.1471	627.4319	643.7870
657.4673	672.0059	695.2970
717.1712	749.2126	753.0341
754.2179	761.7663	774.4354
782.8599	785.5505	831.2281
848.0707	866.9904	868.0377
883.4948	886.9829	898.6767
912.8634	915.2604	933.7757

940.6974	966.9532	971.3234
994.9330	1000.7841	1021.5239
1029.4801	1111.6741	1137.7599
1150.1619	1153.4269	1187.1362
1194.2333	1214.9614	1220.3707
1280.0843	1286.8976	1302.3397
1311.5613	1316.1469	1319.1691
1364.2599	1381.8937	1409.1683
1418.9794	1426.8251	1440.9783
1448.7036	1468.8601	1492.6659
1552.2045	1565.7274	1580.5837
1597.2965	1632.1286	1642.2619
1646.7595	1671.5025	2117.0742
3133.7539	3147.8664	3148.9466
3151.5403	3153.6065	3155.3953
3156.5311	3158.2138	3159.4356
3162.5613	3174.9658	3176.6137
3187.0613	3238.4355	3457.8509

[i1] → P3 + H $C_{22}H_{15}$, C_1, ^2A

6	0	-6.046506	-1.506631	-0.013855
6	0	-4.752177	-1.935603	-0.004890
6	0	-3.665203	-1.002321	0.000242
6	0	-3.971420	0.414503	-0.004332
6	0	-5.346413	0.815399	-0.013789
6	0	-6.348231	-0.109923	-0.018380
6	0	-2.336131	-1.410374	0.009255
6	0	-2.929022	1.335507	0.000530
6	0	-1.580931	0.932279	0.009745
6	0	-1.274105	-0.485256	0.014251
6	0	0.074563	-0.889103	0.023567
6	0	1.117669	0.032721	0.025760
6	0	0.808799	1.448763	0.023890
6	0	-0.517383	1.857767	0.015836
6	0	1.902229	2.374490	0.036357
6	0	2.485677	-0.373026	0.034009
6	0	3.190833	1.940939	0.043597
6	0	3.514966	0.537514	0.033640
6	0	4.933031	0.159668	0.045948
6	0	5.438102	-1.093283	-0.115638
6	0	6.807507	-1.407807	0.010182
6	0	7.972303	-1.708727	0.108258
1	0	0.303930	-1.950250	0.026883
1	0	-2.106911	-2.471573	0.012487
1	0	-6.858773	-2.224630	-0.017676
1	0	-4.522478	-2.995969	-0.001505
1	0	-5.575224	1.875958	-0.017289
1	0	-7.384451	0.208704	-0.025569
1	0	-3.158973	2.396555	-0.002943
1	0	-0.746074	2.919052	0.014294
1	0	1.681683	3.436687	0.040057

1	0	2.692729	-1.437266	0.057210
1	0	4.004515	2.658059	0.047815
1	0	5.394561	0.955725	-1.866724
1	0	5.625949	0.944308	0.334045
1	0	4.781247	-1.915749	-0.384109
1	0	8.999335	-1.964587	0.197930

Frequencies

-522.8350	28.6071	44.1487
62.7161	78.1823	95.5146
137.3255	150.6938	180.4048
191.8957	221.4464	273.8065
283.5861	306.4827	321.8102
330.9317	363.1744	388.2801
395.3982	442.0869	450.6516
470.6610	475.5413	481.6488
501.7846	523.3018	541.9590
571.4222	617.3921	622.6488
629.4162	639.0515	649.5490
680.1006	732.1392	750.7485
757.7538	763.9541	765.3251
775.2870	776.5402	807.2032
844.5377	850.4672	854.6648
856.2301	880.8678	884.4601
897.0051	914.3039	921.9166
929.4667	972.4455	976.8875
984.0761	989.1032	996.4526
1021.9448	1041.6228	1148.8153
1150.4744	1169.2228	1178.3963
1188.2120	1205.6304	1224.0555
1234.7885	1283.0758	1294.4683
1301.0949	1311.4070	1318.7141
1325.1434	1350.9815	1369.9659
1399.0124	1412.6105	1425.3379
1437.7113	1465.1346	1486.2544
1499.9989	1553.6921	1573.8496
1581.4176	1601.7963	1610.1842
1645.9975	1660.4645	1674.7310
2179.8810	3144.1011	3154.5562
3156.2245	3157.1223	3157.4742
3159.1766	3159.7821	3161.4469
3163.6796	3170.3135	3176.0635
3178.6862	3188.0046	3476.0473

[i1] → **[i3]** $C_{22}H_{15}$, C_1, ^2A

6	0	6.313547	-0.727368	-0.149930
6	0	5.131904	-1.407607	-0.131971
6	0	3.880299	-0.712771	-0.072684
6	0	3.896475	0.736182	-0.031940
6	0	5.163134	1.405299	-0.052894
6	0	6.329437	0.701087	-0.109784

6	0	2.660471	-1.379648	-0.053244
6	0	2.691609	1.427848	0.025712
6	0	1.451737	0.760921	0.045767
6	0	1.435210	-0.687786	0.005111
6	0	0.194525	-1.354490	0.025234
6	0	-1.013292	-0.667649	0.081804
6	0	-0.993335	0.785655	0.123272
6	0	0.225263	1.452108	0.104293
6	0	-2.249804	1.491892	0.186363
6	0	-2.273427	-1.356506	0.101077
6	0	-3.383761	0.762060	0.195362
6	0	-3.444045	-0.657218	0.154619
6	0	-4.868174	-1.178204	0.160831
6	0	-6.915548	0.291764	-0.254561
6	0	-7.883894	0.532523	-0.933817
6	0	-5.750370	0.036027	0.525959
1	0	0.184643	-2.439726	-0.005775
1	0	2.648747	-2.464907	-0.083889
1	0	7.252724	-1.267121	-0.194992
1	0	5.119385	-2.492134	-0.162490
1	0	5.174685	2.489834	-0.022453
1	0	7.280382	1.221547	-0.125052
1	0	2.703820	2.513094	0.056087
1	0	0.236249	2.537257	0.135333
1	0	-2.245438	2.576668	0.223624
1	0	-2.268836	-2.442721	0.073760
1	0	-5.141635	-1.550986	-0.830475
1	0	-5.007989	-2.002792	0.865383
1	0	-8.740300	0.738878	-1.527289
1	0	-4.852216	0.928692	0.332073
1	0	-5.931987	0.129708	1.598689

Frequencies

-1650.4336	23.1381	52.4637
68.3682	93.3585	118.8345
139.5673	181.9216	193.2734
228.4217	249.9315	264.0616
292.9738	341.2263	348.8151
375.3196	405.7546	451.3932
458.7435	463.8599	474.1679
479.8409	513.6593	535.9498
544.1038	586.0177	594.8277
622.8584	624.1935	642.8441
654.9253	668.5931	719.9807
746.7851	750.0717	757.4502
762.0842	773.4937	774.9772
818.0373	828.1287	838.6708
845.9222	863.2593	873.8256
880.1710	894.6744	914.6333
919.8806	923.6401	947.6404
959.0062	971.5868	995.3205

1021.6323	1023.4543	1074.7126
1145.3869	1148.4877	1165.5669
1186.1534	1188.1128	1190.8341
1214.8055	1223.2066	1256.3454
1275.4310	1288.5509	1301.1511
1304.0086	1313.2698	1316.5093
1361.8799	1364.8066	1389.2203
1404.8078	1422.9515	1423.2209
1439.7254	1471.1616	1480.1153
1492.8049	1555.5781	1576.7357
1584.3307	1608.1765	1643.9515
1649.8118	1665.0629	1671.9402
2168.7515	3039.3707	3067.8846
3083.5111	3146.0498	3153.6463
3155.1815	3156.2423	3157.2610
3158.4210	3160.0128	3162.8450
3175.2516	3187.3102	3475.3167

[i1] → [i6] $C_{22}H_{15}$, C_1, ^2A

6	0	-5.775931	-1.611779	0.056645
6	0	-4.465510	-1.977101	0.151485
6	0	-3.419601	-1.000841	0.078506
6	0	-3.785318	0.390276	-0.099237
6	0	-5.175169	0.724207	-0.193559
6	0	-6.136401	-0.240191	-0.118563
6	0	-2.075191	-1.343965	0.172083
6	0	-2.783324	1.351802	-0.172477
6	0	-1.419933	1.013967	-0.078568
6	0	-1.053811	-0.377646	0.099422
6	0	0.310454	-0.718673	0.193006
6	0	1.307540	0.245030	0.120253
6	0	0.944565	1.646781	-0.058907
6	0	-0.399539	1.983700	-0.152623
6	0	1.989617	2.629730	-0.133693
6	0	2.698102	-0.018083	0.206182
6	0	3.307927	2.289813	-0.040695
6	0	3.677807	0.916983	0.139255
6	0	5.079973	0.358771	0.249986
6	0	5.552986	-2.111473	-0.198769
6	0	6.085608	-2.944705	-0.891070
6	0	4.887107	-1.134696	0.598092
1	0	0.588727	-1.758759	0.324109
1	0	-1.801628	-2.386153	0.304900
1	0	-6.556438	-2.362097	0.113604
1	0	-4.191463	-3.018459	0.284420
1	0	-5.448158	1.765854	-0.326690
1	0	-7.184401	0.027657	-0.191632
1	0	-3.057104	2.393955	-0.305997
1	0	-0.676590	3.024990	-0.288018
1	0	1.702504	3.667399	-0.267653
1	0	4.077013	3.053634	-0.100267

1	0	5.620074	0.468011	-0.695239
1	0	5.670671	0.872323	1.015731
1	0	6.562116	-3.675989	-1.496338
1	0	3.622698	-1.161910	0.401165
1	0	4.960222	-1.341888	1.667385

Frequencies

-1647.4334	30.5822	47.5051
66.7987	86.0765	120.3163
140.7834	168.9902	216.7272
218.1307	229.9988	288.3275
298.9883	337.8962	356.8214
382.9982	400.0524	432.0087
467.4158	473.1485	477.6987
512.3690	525.0718	530.8918
548.9262	557.5146	580.6905
603.8907	623.9078	640.0540
662.4184	667.6049	728.7965
744.7756	750.3457	756.9799
763.0781	772.7297	774.7516
797.9128	841.5290	846.9252
847.9256	863.2237	883.9245
892.9704	912.2982	915.4677
925.3287	936.0814	970.1555
971.9594	995.6167	997.1163
1019.4081	1021.8542	1074.4490
1143.0460	1150.4981	1150.7964
1182.7059	1187.0488	1194.6546
1207.4075	1221.2679	1249.2391
1272.5633	1287.3321	1297.9889
1304.8869	1318.9933	1334.5918
1356.4978	1360.7816	1388.0518
1405.7302	1414.0525	1428.9122
1455.6140	1479.9028	1485.7579
1494.8442	1547.7285	1558.6493
1581.0532	1607.0295	1645.8216
1655.9559	1665.2843	1673.9740
2167.9924	3030.1485	3060.7153
3084.0660	3151.5955	3153.4066
3155.7616	3157.7721	3158.2705
3162.8670	3170.5896	3172.9611
3175.4463	3187.4314	3475.3424

[i2] → P4 + H $C_{22}H_{15}$, C_1, ^2A

6	0	6.099705	-1.515333	-0.010553
6	0	4.806095	-1.944966	0.028968
6	0	3.718096	-1.013157	0.013569
6	0	4.022154	0.402744	-0.045219
6	0	5.396308	0.804452	-0.085166
6	0	6.399348	-0.119479	-0.068502
6	0	2.389584	-1.421880	0.053177

6	0	2.978489	1.322401	-0.060866
6	0	1.631346	0.918379	-0.021036
6	0	1.326847	-0.498171	0.037923
6	0	-0.021531	-0.902687	0.077994
6	0	-1.064265	0.018188	0.062672
6	0	-0.758835	1.433780	0.003444
6	0	0.566514	1.842795	-0.036324
6	0	-1.851859	2.361870	-0.009512
6	0	-3.142126	1.936990	0.032212
6	0	-3.454613	0.530756	0.085095
6	0	-2.432060	-0.388190	0.103848
6	0	-4.818523	0.102106	0.103518
6	0	-5.904968	-0.407986	-0.120294
6	0	-7.208974	-0.911829	-0.307259
6	0	-7.586151	-2.173847	-0.046059
1	0	-0.250359	-1.962909	0.122280
1	0	2.161759	-2.482451	0.097409
1	0	6.912859	-2.232233	0.001823
1	0	4.577903	-3.004744	0.073087
1	0	5.623567	1.864437	-0.129127
1	0	7.434956	0.199752	-0.099164
1	0	3.206918	2.382864	-0.104885
1	0	0.794136	2.903383	-0.080270
1	0	-1.628450	3.422633	-0.051453
1	0	-3.959733	2.646862	0.027782
1	0	-2.661788	-1.446430	0.149341
1	0	-5.320304	1.054948	1.815946
1	0	-7.940357	-0.207327	-0.697069
1	0	-6.888638	-2.905728	0.343078
1	0	-8.605945	-2.494656	-0.218557

Frequencies

-610.7519	29.6532	36.3939
47.5106	75.2264	97.6815
112.6296	136.6585	150.9355
182.4519	209.1979	234.8378
255.7945	286.6491	308.9728
329.4618	378.0588	394.5747
416.0027	439.7310	469.5832
475.3810	479.8854	483.0120
520.3204	526.7954	544.3154
573.8051	591.5254	626.6296
639.7500	651.1021	686.0013
694.0627	732.4461	750.9519
760.9992	764.6185	765.2566
775.7551	810.9107	813.3475
846.1466	857.2271	870.6015
881.9487	901.1038	911.8235
914.8893	926.1942	936.6275
939.2071	972.4654	981.5925
989.0257	996.4647	999.7627

1022.1391	1094.8942	1150.3697
1150.6331	1164.9618	1188.1495
1203.6282	1218.5712	1223.8706
1262.2947	1292.2784	1298.4903
1315.1462	1316.1665	1321.5478
1335.6124	1368.5256	1392.4180
1411.7760	1424.4268	1434.8417
1446.4643	1463.6245	1486.9558
1499.3004	1550.3821	1569.9643
1581.2393	1608.5519	1639.7548
1645.9220	1657.4196	1673.8148
2214.1889	3130.9223	3147.5469
3154.9171	3156.7318	3157.8244
3159.4404	3160.7855	3163.6924
3166.0444	3176.0433	3180.7152
3187.9724	3195.6815	3238.3995

[i3] → **[i4]** $C_{22}H_{15}$, C_1, ^2A

6	0	6.153523	-0.775120	0.187466
6	0	4.965822	-1.444202	0.147288
6	0	3.722107	-0.737752	0.068739
6	0	3.751744	0.710729	0.032536
6	0	5.023801	1.367942	0.077106
6	0	6.182812	0.652980	0.151845
6	0	2.496099	-1.392951	0.026433
6	0	2.553891	1.413674	-0.043722
6	0	1.308475	0.759094	-0.086769
6	0	1.278988	-0.689670	-0.050536
6	0	0.032068	-1.345256	-0.093969
6	0	-1.165450	-0.644363	-0.170466
6	0	-1.133359	0.804945	-0.206258
6	0	0.088625	1.462117	-0.164216
6	0	-2.391704	1.505611	-0.275084
6	0	-2.433623	-1.313674	-0.215528
6	0	-3.534057	0.793205	-0.329801
6	0	-3.617953	-0.629330	-0.298912
6	0	-4.949167	-1.341178	-0.400712
6	0	-6.086977	0.584822	0.596492
6	0	-5.622008	1.677673	0.316009
6	0	-5.996216	-0.871481	0.648893
1	0	0.011230	-2.430561	-0.067421
1	0	2.473716	-2.478219	0.053430
1	0	7.086801	-1.323680	0.246865
1	0	4.942752	-2.528706	0.174254
1	0	5.045839	2.452443	0.050007
1	0	7.137948	1.164967	0.184816
1	0	2.577001	2.498873	-0.070905
1	0	0.109839	2.547291	-0.191269
1	0	-2.383965	2.592051	-0.278176
1	0	-2.437095	-2.400485	-0.195495
1	0	-5.373389	-1.159450	-1.394323

1	0	-4.801604	-2.419764	-0.301889
1	0	-5.498266	2.728316	0.192644
1	0	-5.694938	-1.184213	1.654534
1	0	-6.960498	-1.345747	0.441920

Frequencies

-369.2739	32.4482	56.2135
79.5668	105.9412	116.5761
156.2314	181.0771	215.6086
247.9548	255.4918	297.4865
327.2985	342.4087	361.7956
374.2255	405.6061	458.2714
465.1845	473.6666	474.4651
479.8417	526.2778	541.1252
549.5925	588.5313	633.8346
645.7422	655.1424	659.3144
716.6280	725.4310	734.2061
749.8798	756.5063	762.7076
766.4765	774.8126	810.2533
825.4926	844.2333	854.1960
858.8773	869.9240	879.3621
893.0667	897.4446	912.9179
919.5259	931.5727	941.7808
970.6282	994.3586	995.9996
1021.9050	1028.3801	1146.4933
1149.1318	1176.9539	1185.8888
1189.3465	1195.2383	1215.4088
1219.2093	1227.0006	1269.1345
1288.5795	1302.4452	1313.4324
1315.5889	1325.6457	1353.9751
1364.5245	1389.0254	1402.8949
1422.1980	1425.4114	1439.6432
1469.2942	1476.2608	1480.8331
1492.6696	1553.6489	1570.9574
1581.4963	1600.8114	1636.0724
1646.8391	1671.3568	2068.9630
3023.4459	3028.0786	3060.8373
3077.1537	3138.9882	3141.3432
3152.6001	3154.5028	3155.6215
3157.4496	3158.5018	3162.0759
3174.6160	3186.7844	3435.3436

[i4] → [i5] $C_{22}H_{15}$, C_1, ^2A

6	0	6.135086	-0.749016	-0.082238
6	0	4.951296	-1.429407	-0.069686
6	0	3.701842	-0.734409	-0.034622
6	0	3.716740	0.712777	-0.012630
6	0	4.981515	1.382281	-0.026928
6	0	6.150183	0.677663	-0.060549
6	0	2.477665	-1.402012	-0.021298
6	0	2.508204	1.404814	0.021334

6	0	1.269937	0.737861	0.035258
6	0	1.256327	-0.711450	0.012837
6	0	0.009756	-1.379653	0.027555
6	0	-1.190119	-0.690819	0.060224
6	0	-1.180134	0.759956	0.082084
6	0	0.041212	1.428816	0.070266
6	0	-2.426539	1.446324	0.094462
6	0	-2.460389	-1.362222	0.090429
6	0	-3.636174	0.776115	0.103297
6	0	-3.635882	-0.681462	0.129138
6	0	-4.971754	-1.386385	0.309269
6	0	-5.977891	0.775741	-0.494457
6	0	-4.915111	1.446071	0.083237
6	0	-6.053218	-0.628671	-0.441183
1	0	0.000362	-2.465409	0.014662
1	0	2.467294	-2.487660	-0.038194
1	0	7.074307	-1.289891	-0.108941
1	0	4.939355	-2.514279	-0.086284
1	0	4.992382	2.467133	-0.010545
1	0	7.100721	1.198999	-0.071110
1	0	2.519718	2.490374	0.037581
1	0	0.050815	2.514319	0.084286
1	0	-2.421779	2.531821	0.076294
1	0	-2.460662	-2.448352	0.113770
1	0	-4.916429	-2.428501	-0.014806
1	0	-5.215820	-1.403926	1.380558
1	0	-4.981792	2.487764	0.378910
1	0	-6.961845	0.146695	0.125624
1	0	-6.701937	-1.156572	-1.136589

Frequencies

-1659.3021	36.6081	67.0578
94.9726	119.7247	139.7610
162.6913	231.7051	238.5063
245.7496	262.8929	335.3205
349.4951	361.9240	387.5767
448.0164	463.4875	469.0719
475.6417	480.4685	492.0172
506.3561	545.7786	556.6647
579.2182	630.1099	645.1762
651.3061	688.9137	722.0055
729.0925	746.5985	750.9009
758.3194	762.8283	767.0556
774.2047	794.3308	816.3602
838.0747	843.3098	846.2540
868.9534	882.1577	887.2978
898.5906	912.2531	919.2697
927.7186	929.4891	969.8164
987.3567	994.2846	1024.4014
1075.8847	1134.9014	1151.9945
1153.6808	1184.6507	1188.0226

1193.9226	1202.0021	1218.4466
1224.6187	1236.1039	1278.7987
1290.9245	1297.7789	1300.8332
1311.3255	1320.4066	1326.4823
1351.8483	1376.4796	1396.1546
1403.4916	1420.4306	1426.4714
1439.4797	1455.1818	1473.3245
1487.7483	1494.5896	1538.0580
1555.4470	1580.0476	1608.2997
1633.9822	1651.7705	1668.8101
2087.2950	2990.5890	3070.2133
3128.1607	3147.5206	3152.9585
3154.7988	3155.6972	3156.3777
3157.8181	3158.0858	3160.7142
3162.7166	3175.0534	3187.2487

[i5] → P1 + H $C_{22}H_{15}$, C_1, ^2A

6	0	6.140128	0.731069	-0.012857
6	0	4.963361	1.417892	-0.028131
6	0	3.705133	0.730080	-0.015870
6	0	3.712097	-0.722122	0.013386
6	0	4.977036	-1.397713	0.028548
6	0	6.147040	-0.699471	0.015920
6	0	2.492054	1.403714	-0.030887
6	0	2.505714	-1.407383	0.025843
6	0	1.263964	-0.734776	0.010859
6	0	1.257145	0.719354	-0.018685
6	0	0.027747	1.392914	-0.033800
6	0	-1.191988	0.708307	-0.021008
6	0	-1.185493	-0.746086	0.008809
6	0	0.041417	-1.419707	0.023684
6	0	-2.422661	-1.429579	0.018142
6	0	-2.436260	1.381823	-0.032234
6	0	-3.634238	-0.754415	0.000366
6	0	-3.638852	0.698063	-0.018687
6	0	-4.910210	1.377280	-0.021226
6	0	-4.891283	-1.441976	-0.019288
6	0	-6.072571	-0.756783	-0.073103
6	0	-6.085010	0.665737	-0.091163
1	0	7.083467	1.265264	-0.022336
1	0	4.957832	2.502644	-0.049832
1	0	4.982009	-2.482467	0.050484
1	0	7.095516	-1.224455	0.027725
1	0	2.487464	2.489169	-0.052563
1	0	2.511494	-2.492829	0.047959
1	0	0.022714	2.478251	-0.054986
1	0	0.046366	-2.505047	0.045661
1	0	-2.419538	-2.515084	0.034473
1	0	-2.441038	2.467355	-0.042667
1	0	-5.065057	1.894543	2.007303
1	0	-4.916801	2.456694	-0.117130

1	0	-4.885301	-2.526773	-0.004613
1	0	-7.012794	-1.295406	-0.103959
1	0	-7.031950	1.190814	-0.137229

Frequencies

-507.2356	36.7277	69.1452
100.7707	118.6211	144.5595
189.4405	221.8939	237.3799
249.1596	260.9301	289.7518
322.8606	350.9988	363.3165
382.9916	454.0280	469.0431
473.5171	477.4774	489.9009
492.7598	512.0279	527.5319
553.5962	579.0628	615.1124
638.5478	646.5660	713.7507
724.5914	744.0873	746.1305
749.5353	756.9671	761.6441
772.0722	776.0202	794.4838
837.2308	839.3083	842.4728
854.3093	874.9076	887.1992
889.0438	900.6316	915.0467
920.5440	921.9470	935.8144
970.5044	972.4183	991.6682
995.4308	1018.5788	1025.1485
1137.4673	1138.4019	1154.4262
1178.2386	1187.2949	1198.7929
1199.7129	1208.3155	1241.0206
1249.3375	1294.5402	1295.0154
1312.0035	1318.3375	1331.6082
1361.4062	1374.9231	1387.2733
1411.8731	1417.9766	1419.4080
1429.0280	1474.8154	1475.5610
1493.0508	1534.8823	1542.5852
1553.0541	1576.4693	1587.7828
1627.7101	1632.5269	1656.2356
1671.3731	3154.4051	3156.0166
3156.2854	3157.9337	3158.3023
3159.8458	3161.1798	3162.0230
3163.6661	3170.4189	3175.8280
3180.0050	3187.7655	3191.1462

[i6] → [i7] $C_{22}H_{15}$, C_1, ^2A

6	0	5.774076	-1.309065	-0.017298
6	0	4.492586	-1.762432	-0.124762
6	0	3.382185	-0.858367	-0.073505
6	0	3.650984	0.556099	0.095762
6	0	5.014257	0.983300	0.204044
6	0	6.039030	0.085378	0.149745
6	0	2.065520	-1.291650	-0.180035
6	0	2.586117	1.448487	0.147290
6	0	1.249251	1.019135	0.039825

6	0	0.979963	-0.395576	-0.128410
6	0	-0.356045	-0.828103	-0.235551
6	0	-1.423323	0.062550	-0.183020
6	0	-1.152379	1.485688	-0.017755
6	0	0.164413	1.916123	0.088965
6	0	-2.265470	2.385178	0.028956
6	0	-2.785485	-0.316430	-0.289595
6	0	-3.547186	1.932856	-0.076971
6	0	-3.844443	0.531907	-0.239786
6	0	-5.284393	0.075567	-0.379260
6	0	-4.663931	-2.153736	0.421294
6	0	-3.532440	-2.511075	0.129432
6	0	-5.665158	-1.101732	0.562073
1	0	-0.552921	-1.885905	-0.367500
1	0	1.864799	-2.351180	-0.306765
1	0	6.604015	-2.005482	-0.057932
1	0	4.291001	-2.821023	-0.251599
1	0	5.214927	2.042070	0.330793
1	0	7.065617	0.423915	0.233126
1	0	2.787569	2.507900	0.273628
1	0	0.366304	2.975904	0.213823
1	0	-2.068574	3.444526	0.154364
1	0	-4.373878	2.636454	-0.041502
1	0	-5.959631	0.913777	-0.186898
1	0	-5.462385	-0.249771	-1.409645
1	0	-2.683051	-3.132694	-0.030556
1	0	-6.669481	-1.458070	0.313656
1	0	-5.693079	-0.765030	1.604388

Frequencies

-380.5410	36.8616	41.5433
83.3018	98.1308	105.7856
156.9114	181.5824	187.0490
245.6970	287.7649	292.0130
323.1155	337.2191	355.7828
388.3203	401.0912	464.7299
471.0947	475.5271	476.7196
497.3021	517.5993	534.1327
557.4962	591.0864	619.7569
635.1332	642.2115	644.2853
716.2171	730.1658	734.6977
749.6334	757.6689	762.3561
770.5036	773.9738	795.9959
806.0008	845.2648	856.1156
857.2655	876.5867	880.0099
904.8198	908.6162	912.1507
932.7779	961.8376	971.1573
984.3283	994.7885	995.0148
1021.0396	1022.3374	1141.9930
1149.1581	1152.6526	1170.3876
1187.6155	1201.8828	1207.1545

1220.2553	1221.8981	1260.9942
1284.9319	1299.4653	1307.9367
1320.8858	1323.2189	1358.6042
1369.4342	1383.2253	1404.7383
1410.1052	1429.0538	1447.1762
1474.3400	1481.9945	1485.8564
1492.4891	1533.5688	1556.2151
1580.4131	1606.1750	1643.8844
1652.5107	1672.4130	2057.5693
3025.3827	3027.1530	3060.1575
3073.7023	3145.8926	3151.5638
3154.3766	3156.6312	3157.5967
3162.1802	3171.9909	3174.7746
3175.0875	3187.0404	3438.3791

[i7] → **[i8]** $C_{22}H_{15}$, C_1, ^2A

6	0	-5.743202	-1.290241	-0.022015
6	0	-4.460168	-1.754894	-0.006276
6	0	-3.348859	-0.853056	-0.002682
6	0	-3.614754	0.570573	-0.016222
6	0	-4.977276	1.010088	-0.032393
6	0	-6.005510	0.113166	-0.035138
6	0	-2.029166	-1.298660	0.013380
6	0	-2.545195	1.461625	-0.014940
6	0	-1.210555	1.017261	0.001983
6	0	-0.944549	-0.405196	0.020012
6	0	0.396270	-0.851126	0.040762
6	0	1.469198	0.026655	0.058478
6	0	1.198989	1.451880	0.007460
6	0	-0.115605	1.903536	-0.012367
6	0	2.301332	2.358757	-0.042714
6	0	2.850979	-0.427319	0.115709
6	0	3.590887	1.898629	-0.036076
6	0	3.884437	0.515480	0.049195
6	0	5.330994	0.062552	0.182538
6	0	4.407886	-2.238739	-0.286510
6	0	3.210884	-1.814581	0.273361
6	0	5.490492	-1.342516	-0.365214
1	0	0.575189	-1.919434	0.024597
1	0	-1.830564	-2.366017	0.023817
1	0	-6.574813	-1.985801	-0.024745
1	0	-4.260260	-2.821287	0.003600
1	0	-5.176105	2.076703	-0.042560
1	0	-7.032253	0.461152	-0.047489
1	0	-2.743670	2.529004	-0.028488
1	0	-0.305734	2.971866	-0.048720
1	0	2.097716	3.422825	-0.094433
1	0	4.413931	2.605269	-0.076108
1	0	6.002042	0.751585	-0.339228
1	0	5.626919	0.102298	1.241756
1	0	2.517233	-2.517021	0.719990

1	0	5.542240	-2.426715	0.374969
1	0	6.323082	-1.567660	-1.028935

Frequencies

-1587.0004	43.1387	57.8186
98.7375	115.1176	122.2079
173.2746	186.5964	232.4095
268.5164	291.3322	299.7977
341.7175	375.0500	395.7581
437.1176	467.0842	473.0975
478.4305	490.1924	502.4281
521.7717	539.6929	556.9071
594.4577	615.8846	622.9841
642.1552	676.9057	705.1831
725.0625	745.1656	750.6918
754.1552	763.0414	770.6828
774.5583	798.5681	802.6075
847.4153	849.3518	857.9812
867.0026	886.2910	910.0667
912.5839	919.9718	928.8373
946.3848	962.6625	970.8804
995.0055	995.6379	1023.3298
1076.0116	1108.1423	1150.8851
1152.4394	1182.3080	1188.7533
1193.2591	1204.6649	1220.2962
1221.9820	1231.6837	1255.1847
1279.2639	1289.4722	1303.3821
1310.3190	1318.4974	1345.5827
1360.2421	1374.7857	1385.0564
1409.8054	1422.7049	1427.3555
1437.4282	1456.3463	1458.4035
1483.1373	1499.7783	1529.3009
1556.1992	1580.5395	1590.3846
1625.6318	1643.5283	1669.5026
2097.1774	2968.2018	3050.0481
3120.1491	3152.7203	3154.1562
3156.0443	3157.6088	3158.4583
3162.6724	3166.1951	3174.7751
3175.1867	3184.8131	3187.2757

[i8] → P2 + H $C_{22}H_{15}$, C_1, ^2A

6	0	5.754258	-1.279499	0.027686
6	0	4.472659	-1.749167	0.029499
6	0	3.358633	-0.851493	0.014363
6	0	3.619011	0.571958	-0.002959
6	0	4.978970	1.017145	-0.004193
6	0	6.011074	0.124151	0.010576
6	0	2.039428	-1.301884	0.015831
6	0	2.544589	1.459417	-0.017556
6	0	1.214730	1.008688	-0.016101
6	0	0.953850	-0.411801	0.000809

6	0	-0.388397	-0.861641	0.001333
6	0	-1.464838	0.006427	-0.013043
6	0	-1.196051	1.430822	-0.027006
6	0	0.110474	1.888636	-0.029197
6	0	-2.300858	2.353943	-0.035080
6	0	-2.860789	-0.446854	-0.013997
6	0	-3.582253	1.920767	-0.025537
6	0	-3.900329	0.518057	-0.013381
6	0	-5.255254	0.090967	0.018946
6	0	-3.220428	-1.808780	-0.034346
6	0	-4.548590	-2.211194	-0.072484
6	0	-5.572542	-1.266620	-0.067635
1	0	6.588438	-1.971856	0.039361
1	0	4.276851	-2.816283	0.042618
1	0	5.173688	2.084447	-0.017084
1	0	7.036419	0.476355	0.009507
1	0	1.845038	-2.370062	0.028922
1	0	2.738805	2.527539	-0.030120
1	0	-0.548772	-1.932648	0.015660
1	0	0.294254	2.958555	-0.039893
1	0	-2.078508	3.415690	-0.045819
1	0	-4.402232	2.630947	-0.022147
1	0	-5.647029	0.366464	1.895907
1	0	-6.033379	0.835827	-0.102013
1	0	-2.451644	-2.570396	-0.039659
1	0	-4.786447	-3.268038	-0.113602
1	0	-6.609585	-1.578806	-0.100794

Frequencies

-679.0496	43.1891	52.7166
100.0731	119.2741	140.0231
186.0739	218.2231	232.5603
271.1715	291.4544	301.0155
326.4499	365.0772	383.9442
395.5388	458.2065	459.2267
471.3190	478.2455	483.4254
517.4374	530.5563	548.3429
558.7254	564.7446	599.8253
638.8468	646.1817	687.1669
724.1378	745.2108	751.1356
751.7991	757.4249	767.6502
774.5719	798.9158	805.1361
815.8268	847.8978	849.5772
862.5412	881.4540	888.6318
894.0884	910.3581	914.7979
930.3083	967.7166	971.2374
981.8082	995.8891	996.7283
1006.0048	1024.7109	1064.4004
1120.9785	1150.4390	1156.7469
1169.9687	1186.8743	1189.9534
1207.7480	1221.7778	1226.8179

1252.2588	1267.2509	1297.6535
1305.9110	1317.5003	1324.5645
1341.0236	1374.0334	1382.0873
1415.7646	1425.1368	1443.9633
1446.7594	1467.6736	1479.4096
1497.8583	1524.0678	1561.7614
1582.8487	1585.1342	1610.6751
1622.8530	1650.7397	1654.2670
1671.6550	3154.3591	3155.6193
3157.4164	3158.2422	3160.0491
3163.0344	3165.6658	3172.0534
3175.5522	3177.5076	3180.2521
3187.6442	3189.7720	3201.0641

References

[1] a) L. Zhao, et al., *ChemPhysChem* **2019**, *20*, 1437; b) L. Zhao, et al., *J. Phys. Chem. Lett.* **2018**, *9*, 2620; c) L. Zhao, R. I. Kaiser, B. Xu, U. Ablikim, M. Ahmed, M. M. Evseev, E. K. Bashkirov, V. N. Azyazov, A. M. Mebel, *Nat. Astron.* **2018**, *2*, 973; d) L. Zhao, R. I. Kaiser, B. Xu, U. Ablikim, M. Ahmed, D. Joshi, G. Veber, F. R. Fischer, A. M. Mebel, *Nat. Astron.* **2018**, *2*, 413; e) L. Zhao, R. I. Kaiser, B. Xu, U. Ablikim, M. Ahmed, M. M. Evseev, E. K. Bashkirov, V. N. Azyazov, A. M. Mebel, *Angew. Chem. Int. Ed.* **2019**, *59*, 4051; *Angew. Chem.* **2020**, *132*, 4080; f) T. Yang, R. I. Kaiser, T. P. Troy, B. Xu, O. Kostko, M. Ahmed, A. M. Mebel, M. V. Zagidullin, V. N. Azyazov, *Angew. Chem. Int. Ed.* **2017**, *56*, 4515; *Angew. Chem.* **2017**, *129*, 4586.

[2] a) Y. Y. Li, L. D. Zhang, Z. Y. Tian, T. Yuan, J. Wang, B. Yang, F. Qi, *Energy Fuels* **2009**, *23*, 1473; b) Y. Y. Li, L. D. Zhang, Z. Y. Tian, T. Yuan, K. W. Zhang, B. Yang, F. Qi, *Proc. Combust. Inst.* **2009**, *32*, 1293; c) P. Oßwald, H. Güldenberg, K. Kohse-Höinghaus, B. Yang, T. Yuan, F. Qi, *Combust. Flame* **2011**, *158*, 2; d) F. Qi, *Proc. Combust. Inst.* **2013**, *34*, 33; e) F. Qi, R. Yang, B. Yang, C. Q. Huang, L. X. Wei, J. Wang, L. S. Sheng, Y. W. Zhang, *Rev. Sci. Instrum.* **2006**, *77*, 084101; f) B. Yang, et al., *Proc. Combust. Inst.* **2007**, *31*, 555; g) B. Yang, P. Oßwald, Y. Li, J. Wang, L. Wei, Z. Tian, F. Qi, K. Kohse-Höinghaus, *Combust. Flame* **2007**, *148*, 198; h) L. D. Zhang, J. H. Cai, T. C. Zhang, F. Qi, *Combust. Flame* **2010**, *157*, 1686.

[3] M. Zagidullin, R. Kaiser, D. Porfiriev, I. Zavershinskiy, M. Ahmed, V. Azyazov, A. Mebel, *J. Phys. Chem. A* **2018**, *122*, 8819.

[4] a) A. G. Baboul, L. A. Curtiss, P. C. Redfern, K. Raghavachari, *J. Chem. Phys.* **1999**, *110*, 7650; b) L. A. Curtiss, P. C. Redfern, K. Raghavachari, V. Rassolov, J. A. Pople, *J. Chem. Phys.* **1999**, *110*, 4703; c) L. A. Curtiss, K. Raghavachari, P. C. Redfern, A. G. Baboul, J. A. Pople, *Chem. Phys. Lett.* **1999**, *314*, 101.

[5] M. J. Frisch, et al., *Gaussian 09, Revision A.1 Gaussian Inc., Wallingford CT* **2009**.

[6] H. J. Werner, et al., *MOLPRO, version 2010.1*, http://www.molpro.net **2010**, *(University College Cardiff Consultants Ltd, United Kingdom)*.

[7] a) Y. Hidaka, K. Tanaka, M. Suga, *Chem. Phys. Lett.* **1986**, *130*, 195; b) Y. Hidaka, H. Masaoka, H. Oshita, T. Nakamura, K. Tanaka, H. Kawano, *Int. J. Chem. Kinet.* **1992**, *24*, 871.

[8] a) C. Kitamura, N. Taka, T. Kawase, *Res. Chem. Intermed.* **2013**, *39*, 139; b) M. Watanabe, T.-H. Chao, C.-T. Chien, S.-W. Liu, Y. J. Chang, K.-Y. Chen, T. J. Chow, *Tetrahedron Lett.* **2012**, *53*, 2284.

[9] a) T. R. Criswell, B. H. Klanderman, *J. Org. Chem.* **1974**, *39*, 770; b) C. Sanchez-Sanchez, et al., *J. Am. Chem. Soc.* **2017**, *139*, 17617.

[10] D. Kato, H. Sakai, N. V. Tkachenko, T. Hasobe, *Angew. Chem. Int. Ed.* **2016**, *55*, 5230; *Angew. Chem.* **2016**, *128*, 5316.

[11] D. J. Pollart, B. Rickborn, *J. Org. Chem.* **1986**, *51*, 3155.

[12] D. García, F. Foubelo, M. Yus, *Tetrahedron* **2008**, *64*, 4275.

[13] G. W. Gribble, E. J. Holubowitch, M. C. Venuti, *Tetrahedron Lett.* **1977**, *18*, 2857.